BRNO UNIVERSITY OF TECHNOLOGY

VYSOKÉ UČENÍ TECHNICKÉ V BRNĚ

FACULTY OF ELECTRICAL ENGINEERING AND COMMUNICATION

FAKULTA ELEKTROTECHNIKY
A KOMUNIKAČNÍCH TECHNOLOGIÍ

DEPARTMENT OF RADIO ELECTRONICS

ÚSTAV RADIOELEKTRONIKY

FILTERING ANTENNA BASED ON COAXIAL CAVITY RESONATORS

FILTRUJÍCÍ ANTÉNA Z KOAXIÁLNÍCH DUTINOVÝCH REZONÁTORŮ

MASTER'S THESIS
DIPLOMOVÁ PRÁCE

AUTHOR
AUTOR PRÁCE

Bc. Ivan Maro

SUPERVISOR
VEDOUCÍ PRÁCE

prof. Dr. Ing. Zbyněk Raida

BRNO 2023

BRNO UNIVERSITY OF TECHNOLOGY
FACULTY OF ELECTRICAL ENGINEERING AND COMMUNICATION

Master's Thesis

Master's study program **Electronics and Communication Technologies**

Department of Radio Electronics

Student: Bc. Ivan Maro ***ID:*** 197722

Year of study: 2 ***Academic year:*** 2022/23

TITLE OF THESIS:

Filtering antenna based on coaxial cavity resonators

INSTRUCTION:

A filtering antenna, which is conceived as an open-ended waveguide, should be studied. The input filter should be created in the feeder using stubs. The waveguide should be fed by a coaxial probe. In a proper electromagnetic simulator, a filtenna model should be developed and correctness of results published in [1] should be verified. Parameters of the filtenna should be improved by replacing the open-ended waveguide by a horn.

The described antenna structure should be modified so that the conventional waveguide can be replaced by a substrate-integrated one. The antenna should be optimized for HIPERLAN frequency band (17 GHz). The optimized antenna should be manufactured and parameters should be verified experimentally. Measurement outputs should be compared with simulations.

RECOMMENDED LITERATURE:

[1] Kai-Ran Xiang; Fu-Chang Chen; Qing-Xin Chu; A Tunable Filtering Antenna Based on Coaxial Cavity Resonators. IEEE Transactions on Antennas and Propagation, 2022, vol. 70, no. 5, p. 3259-3268. DOI: 10.1109/TAP.2021.3137516

[2] C. A. Balanis; Antenna Theory: Analysis and Design, 4th Edition. Hoboken: John Wiley & Sons, 2016. ISBN: 978-1-1186-4206-1

Date of project specification: 6.2.2023 ***Deadline for submission:*** 22.5.2023

Supervisor: prof. Dr. Ing. Zbyněk Raida

doc. Ing. Lucie Hudcová, Ph.D.
Chair of study program board

WARNING:

The author of the Master's Thesis claims that by creating this thesis he/she did not infringe the rights of third persons and the personal and/or property rights of third persons were not subjected to derogatory treatment. The author is fully aware of the legal consequences of an infringement of provisions as per Section 11 and following of Act No 121/2000 Coll. on copyright and rights related to copyright and on amendments to some other laws (the Copyright Act) in the wording of subsequent directives including the possible criminal consequences as resulting from provisions of Part 2, Chapter VI, Article 4 of Criminal Code 40/2009 Coll.

Abstract

This semestral thesis is aimed at verifying the functionality of the proposed concept of a tuneable filtering antenna. The antenna is designed in such way that it combines the filtering and radiating functions into a single unit. After simulating and verifying the correct functionality of the proposed antenna [1] in an electromagnetic simulator, thesis than discusses the possibilities of improving the antenna parameters. To achieve higher directivity and gain, a solution is proposed where a pyramidal horn antenna is added at the end of the filtering waveguide. Obtained results are than used to design antenna integrated into substrate.

Keywords

waveguide, cavity resonator, tuneable filtering antenna, SIW, horn antenna, dielectric loading

Abstrakt

Táto práca je zameraná na overenie funkčnosti navrhnutého konceptu laditeľnej filtračnej anténny. Anténa je navrhnutá tak aby spájala filtračnú a vyžarovaciu funkciu do jedného celku. Po odsimulovaní a overení správnej funkčnosti navrhovanej anténny [1] v elektromagnetickom simulátore, sa práca zaoberá možnosťami vylepšenia parametrov anténny. Na dosiahnutie vyššej smerovosti a zisku je navrhnuté riešenie kedy je na koniec filtračného vlnovodu pridaná pyramídová horn anténna. Obdŕžane výsledky sú následne použité pre navh antény integrovanej do subtrátu.

Klíčová slova

vlnovod, dutinový rezonátor, filtrujúca laditeľná anténa, SIW, horn anténa, dielektrická záťaž

Rozšířený abstrakt

S neustálym vývojom bezdrôtových technológii, narastajú nároky na čoraz väčšiu miniaturizáciu a integráciu rádiofrekvenčných (RF) obvodov. V minulosti bolo potrebne navrhovať pasívne prvky ako sú: anténny, filtre, duplexový ako individuálne bloky ktoré boli medzi sebou následne spájane pomocou 50 ohmového vedenia. Tento prístup je veľmi náročne replikovať pri stále sa zväčšujúcich nárokoch na miniaturizáciu. Prechod signálu veľkým množstvom blokov taktiež negatívne ovplyvňuje bitovú chybovosť (BER) a zhoršuje pomer SNR. Na riešenie týchto problémov sa v poslednej dobe čoraz častejšie uplatňuje spájanie blokov do väčších celkov, čo však zo sebou nesie ďalšie problémy. Pre zlepšenie selektivity týchto systémov sa často krát používajú filtračne antény kde je pomocou rezonátor vo forme cylindrov alebo výrezov (slots) realizovaný výstupný filter. Použitie rezonátu ma za účel dosiahnuť slabú väzbu medzi napájaním antény a vyžarovacím elementom. Anténny s integrovaným filtrom dosahujú väčšej selektivity a úroveň potlačenie nechcených signálov mimo pracovného pásma, ako konvenčne používané antény. Vďaka ich schopnostiam potlačovať signály mimo požadované pásmo sú filtračne antény vhodne pre použitie vo viacpásmových systémoch, kde prispievajú k lepšej izolácii medzi jednotlivými rádiovými službami bez toho, aby navyšovali rozmery antény. Táto práca predstavuje stručný úvod do problematiky a návrhu filtračných antén na bazé dutinových vlnovodou a vlnvodoch integrovaných do substrátu.

Bibliographic citation

MARO, Ivan. *Filtrující anténa z koaxiálních dutinových rezonátorů* [online]. Brno, 2023 [cit.2022-12-31].Dostupnéz: https://www.vutbr.cz/studenti/zav-prace/detail/144294. Semestrální práce. Vysoké učení technické v Brně, Fakulta elektrotechniky a komunikačních technologií, Ústav radioelektroniky. Vedoucí práce Zbyněk Raida.

Author's Declaration

Author:	*Ivan Maro*
Author's ID:	*197722*
Paper type:	*Master's Thesis*
Academic year:	*2022/23*
Topic:	*Filtering antenna based on coaxial cavity resonators*

I declare that I have written this paper independently, under the guidance of the advisor and using exclusively the technical references and other sources of information cited in the project and listed in the comprehensive bibliography at the end of the project.

As the author, I furthermore declare that, with respect to the creation of this paper, I have not infringed any copyright or violated anyone's personal and/or ownership rights. In this context, I am fully aware of the consequences of breaking Regulation S 11 of the Copyright Act No. 121/2000 Coll. of the Czech Republic, as amended, and of any breach of rights related to intellectual property or introduced within amendments to relevant Acts such as the Intellectual Property Act or the Criminal Code, Act No. 40/2009 Coll., Section 2, Head VI, Part 4.

.

Brno, May 22, 2023 ----------

author's signature

Acknowledgement

I would like to thank my thesis supervisor, prof. Dr. Ing. Zbyněk Raida for effective methodological, pedagogical, and professional help and other valuable advice during the preparation of my master's thesis.

.

Brno, May 22, 2023

Author's signature

Contents

FIGURES

TABLES

INTRODUCTION

Aim of this thesis was to verify functionality and method of implementation of filtering waveguide antennas which are designed as open-ended waveguide. Input waveguide filter should be implemented by means of tuning stubs and fed by a coaxial probe. Initial antenna model on which the work is based is given in reference [1]

This master thesis theses can be split into two main parts, filtering horn antenna based on rectangular waveguide and second half which describe process of designing and manufacturing of filtering antenna integrated into substrate.

First chapet briefly deals with an introduction to the problem of waveguides. Reader is also familiarised with waveguide design and standards used in practice.

Second chapter focuses on the topic of filtering antennas, their gradual design from passive resonators to waveguide filters.

Third chapter is devoted to the core of master thesis, which is the verification of the functionality of the proposed open waveguide filter antenna for use in the frequency band 9 to 11 GHz. An electromagnetic simulator was used to replicate antenna model, and the findings were compared to those reported in [1].

Fourth chapter discusses the possibilities of improving third order filtering antenna parameters [1] by adding horn antenna to the end of the open waveguide. Factors under consideration include gain, directivity and antenna selectivity while preserving original filtering properties of antenna.

The fifth chapter deals with the step-by-step design of a tuneable antenna integrated into a substrate, taking advantage of the similarities and knowledge gained from the design of the tuneable antenna in the chapter 3.

Second to last chapter describes the way of manufacturing the antenna integrated into the substrate designed in chapter 5 as well as the modifications needed to manufacture the antenna.

Last chapter briefly highlights the process of measuring manufactured antenna's parameters, including its radiation pattern and the gain. The results are then compared with those obtained from the CST electromagnetic simulator.

1. WAVEGUIDE ANTENNAS

An open-ended waveguide serves as the foundation of a waveguide antenna.
These days, antennas of this kind are frequently used, particularly in radar and navigation systems. Their straightforward, durable design and affordable production are their key features as well as their ability to transmit high power signals up to several megawatts is also possible with this sort of antenna. The waveguide's dimensions determines whether the antenna emits a linear or circular polarization.

1.1 Waveguides

A waveguide is type of electromagnetic energy transmission line. It is mainly used in the higher frequency range. Since its losses are significantly lower in this region compared to coaxial or microstrip lines [2]. By waveguide we usually mean a hollow metal tube of various shapes (Fig. 1.1), but in practice two types are mainly used, namely waveguide with circular (Fig. 1.1 (b)) and rectangular (Fig. 1.1 (a)) cross-section. Internal dimensions of the waveguide also determine the condition under which an electromagnetic wave can propagate inside the waveguide.

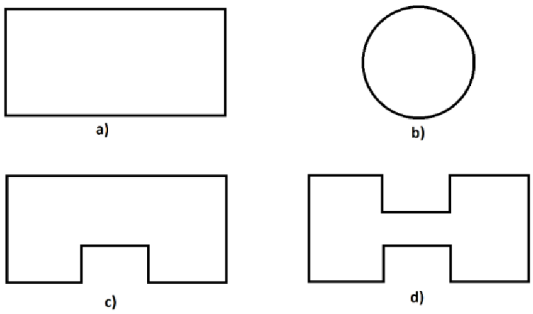

Fig. 1.1 Waveguide cross-section: a) rectangular, b) circular, c) single ridged, d) double ridged

Bandwidth of a waveguide is characterized by its passband it is the frequency band in which the signal is transmitted with minimum attenuation. Passband is limited at the bottom by the cut-off frequency of the lowest mode, which is dependent on the transverse dimensions of the waveguide and does not depend on the waveguide length. A wave of lower frequency than the cut-off frequency cannot propagate through the waveguide [2]. The parameter that also characterizes waveguide is the phase velocity of the wave in the waveguide. It defines the speed with which the locations of constant phase of signal are moving. The wave's length in the waveguide represents the distance it will travel at phase

speed in one cycle of the signal. This length can be calculated as shown in (Equation 1.1) .Where $\lambda_g$represents length of wave in waveguide, while λ determine length of wave in free space.

$$\lambda_g = \frac{\lambda}{\sqrt{1-\left(\frac{\lambda}{\lambda_c}\right)^2}} \tag{1.1}$$

The last parameter that characterizes waveguide is its attenuation [2]. We recognize three types of attenuation, namely the attenuation of the waveguide due to imperfectly conducting walls characterized by the penetration depth. Additionally, attenuation due to dielectric losses and attenuation due to reflection at the waveguide feeding port.

1.2 Design of a waveguide with rectangular cross-section

An infinite number of modes, labelled as TE (Transversal electric) and TM (Transversal magnetic), can propagate through the waveguide [2]. These modes are always represented in the form TEmn/ TMmn. Where (*m*) and (*n*) are non-zero integers, for the TE mode (*m*) can also be zero. We calculate the cut-off frequency *fc* of a rectangular waveguide as:

$$f_c = TE_{m,n} = \frac{c}{\sqrt{\varepsilon_r \mu_r}} \sqrt{\left(\frac{m}{2a}\right)^2 + \left(\frac{n}{2b}\right)^2} \tag{1.2}$$

Different modes differ from each other in their cut-off frequency, phase velocity, and hence the change in wavelength in the waveguide (Equation 1.1) Waveguides are often designed to operate in single-mode region. This eliminates dispersion of transmitted signals due to different phase velocities. In a rectangular waveguide, we can determine the wavelength of the dominant TE_{10} mode according to equation (1.3) [2]. An important factor in waveguide design is the ratio of the shorter and longer sides of the waveguide. This ratio is directly dependent on the shortest and longest wavelength that can propagate in a given waveguide. The most commonly used aspect ratio in practice is 2:1.

$$\lambda_c^{TE10} = 2\mathrm{a} \tag{1.3}$$

Rectangular waveguide that will be used later in Chapter 3 operates in the 9-12GHz frequency range. Therefore, the upper frequency of the dominant mode TE10 is taken into consideration for the calculation. Equation (1.2) will simplify into the form:

$$f_c^{TE10} = \frac{\pi}{2a\pi\sqrt{\varepsilon\mu}} \tag{1.4}$$

Equation (1.4) can be further simplified by using mathematical formula (1.5) [2]

$$c = \frac{1}{\sqrt{\varepsilon\mu}} \tag{1.5}$$

We will obtain an equation in the form:

$$f_c^{TE10} = \frac{c}{2a} \tag{1.6}$$

From equation (1.6) we can express the relation for the longer side (a) of rectangular waveguide as: (1.7)

$$a = \frac{c}{2f_c^{TE10}} \tag{1.7}$$

The cut-off frequency in waveguide design for a given frequency range is usually chosen as half of the desired upper frequency. For the calculation of approximate dimensions of waveguide, a cut-off frequency of 6 GHz was chosen. From the known frequency we can calculate the longer of waveguide sides as:

$$a = \frac{c}{2f_c^{TE10}} = \frac{3 \cdot 10^8}{2 \cdot 6 \cdot 10^8} = 25\ mm \tag{1.8}$$

From known side (a) we can calculate cut-off frequency of the next mode TE_{20} (Equation 1.10), This frequency simultaneously gives the upper frequency limit for waveguide in order to work in single-mode region. Frequencies used in the waveguide must also satisfy condition (1.9).

$$f_c^{TE20} < f < f_c^{TE10} \tag{1.9}$$

$$f_c^{TE20} = \frac{c}{a} = \frac{3 \cdot 10^8}{25 \cdot 10^{-3}} = \ 12\ GHz \tag{1.10}$$

Ratio of the critical frequency and frequency from which the TE_{20} mode starts to propagate gives us the aspect ratio of rectangular waveguide in our case it is 2:1. Wavelengths that will propagate through the waveguide fall in the range of 25 to 50 mm.

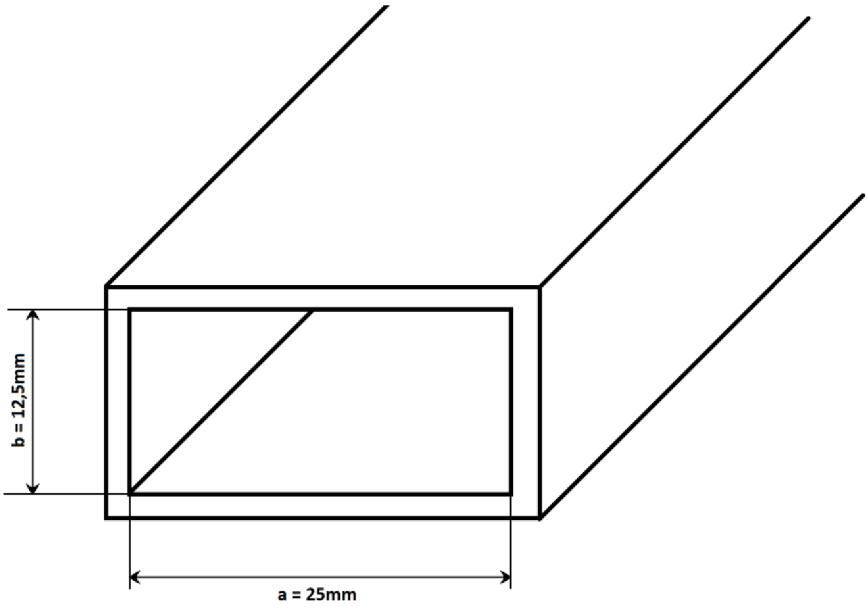

Fig. 1.2 Designed theoretical rectangular waveguide

The last step in the design is to calculate wavelength at the operating frequency inside the waveguide in order to achieve efficient excitation of electromagnetic field in the waveguide. For operating frequency of 10 GHz, wavelength is calculated using equation (1.11)

$$\lambda_g = \frac{\lambda}{\sqrt{1-\left(\frac{\lambda}{\lambda_c}\right)^2}} = \frac{29{,}979 \cdot 10^8}{\sqrt{1-\left(\frac{29{,}979 \cdot 10^8}{50 \cdot 10^8}\right)^2}} = 30{,}4\,mm \tag{1.11}$$

1.3 Standardisation of waveguide dimensions

As already mentioned in chapter 1.1 transverse dimensions of the waveguide define the frequency band in which the waveguide can be used. As shown in chapter 1.2 dimensions of the waveguide can be theoretically calculated for any frequency band. However, in practice a set of waveguides with standardised dimensions is used. Standardising waveguide dimensions allows us to integrate waveguides from different manufacturers and ensures interface compatibility. It also allows user to integrate waveguide of known parameters into the design of the proposed system. Most well-known and widely used standards include IEEE (Institute of Electrical and Electronics Engineers), MIL (United States Military), EIA (Electronic Industries Alliance Standards), IEC (International Electrotechnical Commission). The most used labelling of waveguides includes the

WR—series of waveguides. Where WR indicates that it is a rectangular waveguide. Following number denotes longer dimension of the waveguide cross-section and is given in units of mils/10. Several examples of waveguides used in practice are shown in (Table 1.1) [3]

Table 1.1 Dimensions of commercially produced waveguides [3] compared with dimension of calculated waveguide

Waveguide name		Recommended frequency	Cut-off frequency lowest order mode	Cut-off frequency next mode	Inner dimensions of waveguide opening	
EIA	IEC	[GHz]	[GHz]	[GHz]	A inch [mm]	B inch [mm]
WR340	R26	2.20 to 3.30	1.736	3.471	3.4 [86.36]	1,7 [43,18]
WR137	R70	5.85 to 8.20	4.301	8.603	1.372 [34.8488]	0,622 [15,7988]
WR90	R100	8.20 to 12.40	6.557	13.114	0.9 [22.86]	0,4 [10,16]
WR10	R900	75 to 110	59.015	118.03	0.1 [2.54]	0,05 [1,27]
Výpočet		7,5 to 11,3	6	12	[25]	[12.5]

Transition between the passband and rejection band of the waveguide is very steep. Measured attenuation of a real waveguide at frequencies just below the cut-off frequency can reach several hundred dB/m. Just above the cut-off frequency, attenuation can be measured in fractions of dB/m. This parameter must also be taken into consideration when selecting appropriate waveguide If the frequency of interest is too close to the operating frequency limit of the waveguide, signal will be also attenuated.

For the values calculated from chapter 1.2 the WR90 waveguide is the most suitable for our requirements, a comparison of its parameters with the calculated values is shown in Table 1.1

2. FILTERING ANTENNAS

As the name suggests, this type of antenna combines filtering and radiation functions in one unit. Direct coupling of the antenna and filter usually introduces a mismatch and reduces the efficiency of the filter. A matching network is inserted between the antenna and the filter to minimize these effects. However, this increases system size, weight, and complexity. The more processing blocks a signal need to pass through, the more it gets distorted. Therefore, filtering antennas are often used to remove matching network (Fig. 2.1).

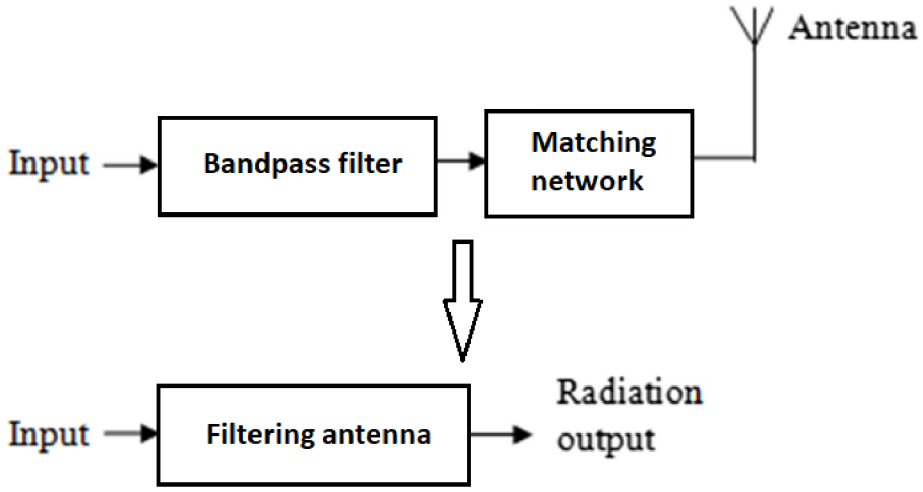

Fig. 2.1 Block diagram of filtering antenna

A major problem today is overcrowding of the frequency bands used in wireless communications. Using an antenna that can be tuned to the operating frequency ensures that transmissions always take place on available frequencies. We can also adjust the antenna bandwidth to better suit our application.

2.1 Microwave Filter

Microwave filters are an integral part of modern communication systems working with microwave frequencies. Filters can be defined as frequency selective networks with two or more ports that are used to pass signals at selected frequencies and attenuate other signals, mostly by reflecting them. A general requirement of modern applications and systems is to reduce weight and minimize size, while maintaining filtering properties [2]. Design of waveguide filters require transmission of signals with large amplitude while maintaining losses as low as possible.

One of the objectives of the work is to validate use of waveguide filters. Waveguide filters can be implemented in several different ways. Many solutions based on modifying rectangular waveguide were proposed in [8] [9] using tuning stubs and embedded iris, these types of filters are well known and used in a wide range of applications. Discontinuities inserted into the waveguide can have different shapes and positions, which are discussed in more detail in section (2.3)

2.2 Resonators

The resonator is characterized as one of the basic passive microwave components used in frequency selective circuits such as filters. Special type of resonator is cavity resonator, which can store frequency-dependent electromagnetic energy. Under ideal conditions, there is no loss in the resonator and electromagnetic field can be stored inside the resonator. However, in real use, resonator loses energy due to losses inside dielectric and conductor or due to coupling with other electrical components. For this reason, energy must be continuously supplied to the circuit. Main parameter of a resonator is its resonant frequency and quality factor also known as Q-factor, which determines the performance of the resonator [10]. For applications at low frequencies up to 1 GHz, resonators are constructed using LC circuits, while for frequencies in the range of to 100 GHz, waveguide resonators are used.

2.3 Construction of waveguide filter

Filtering function of the waveguide can be achieved by adding elements to the cavity of the waveguide [9]. Shape and position of the inserted element always depends on particular filter application. Use of the filter also predetermines its desired parameter, centre frequency, bandwidth, as well as attenuation in passband and rejection band. Waveguide filter can be described by an equivalent circuit (Fig. 2.2), where K represents one of the coefficients of transfer function.

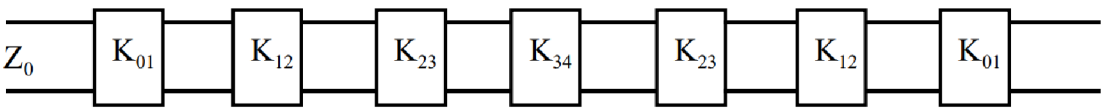

Fig. 2.2 Equivalent circuit of waveguide filter [4]

Design of waveguide filter start by inserting simple elements into cavity of waveguide. Elements inserted into the waveguide, form a barrier to the propagating electromagnetic waves between the two ports. This creates resonance points which form zeros in transfer function. In practice, iris or inductive posts are most commonly used as obstacles (Fig 2.3). By changing their dimensions and position in the waveguide we can achieve our desired filter parameters. For this semester project, the method of

implementation using inductive pins was chosen. This method allows easy and fast tuning of the frequency band, later inductive pins can be replaced by tuning screws with fine thread. Disadvantage of this implementation is that the distance between the pins is fixed and cannot be changed.

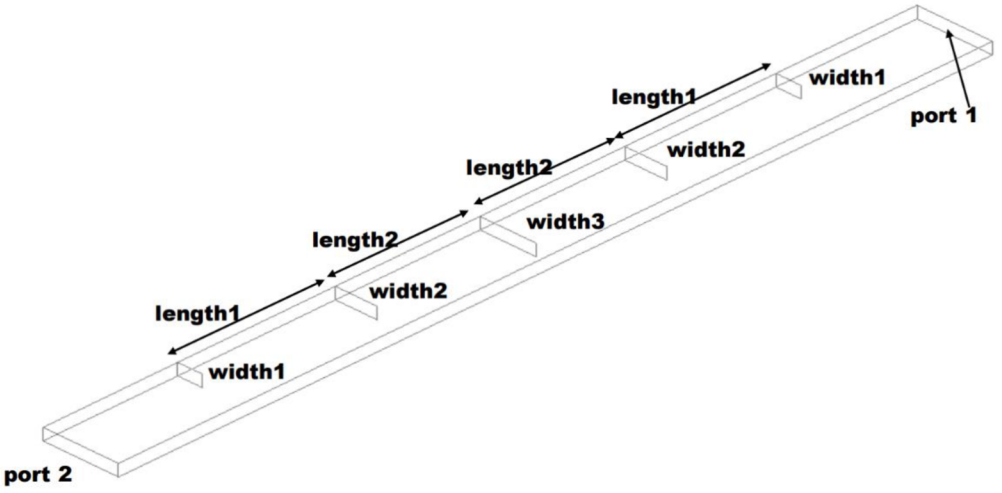

Fig. 2.3 Resonators inserted into waveguide [4]

-

3. OPEN ENDED WAVEGUIDE ANTENNA

Summarizing the previous chapters, we get an open-ended antenna. This type of antenna is widely used in practice. It consists of a waveguide which is opened on one side. Many articles have dealt with this type of antenna and its variations. Following chapter is aimed at verifying the functionality of proposed antenna published in research paper [1].

3.1 Cavity resonator antenna

Body of an antenna consists of a cavity resonator, in which we can store electromagnetic energy under ideal conditions. We can control resonant frequency inside cavity by extending and retracting a metal cylinder h_c into the resonator cavity as shown by (Fig. 3.1), or by changing the dimensions *a,b,w* of resonant cavity. During the manufacture of the antenna, cylinder is replaced by a tuning screw with a fine thread. Quality factor of resonator is influenced by the resonant cylinder diameter, the higher the quality factor, the lower the antenna loss.

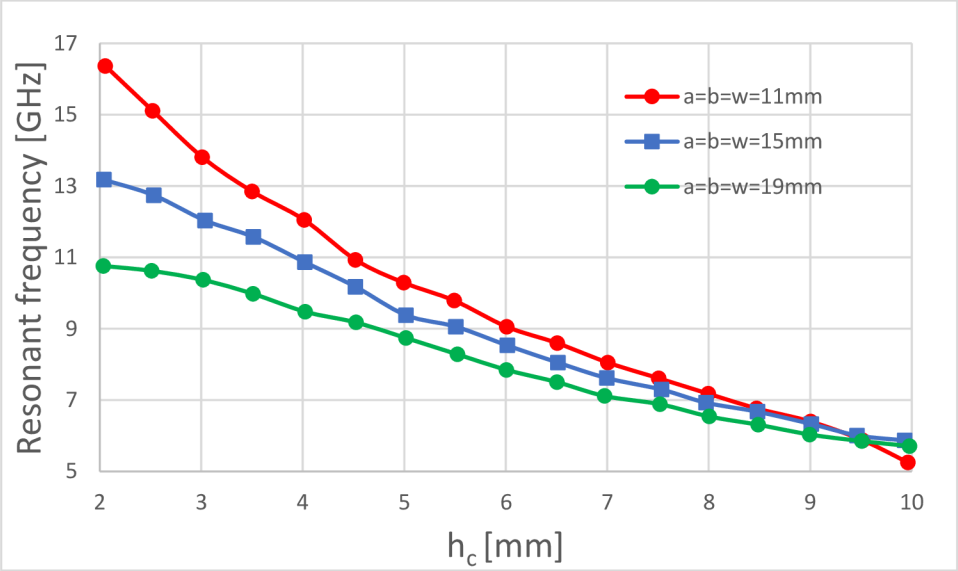

Fig. 3.1 Resonant frequency under different parameters [1]

By cutting holes for coupling and radiating slot in the direction of "Z" axis into the cavity resonator, we get a simple model of filtering antenna. Cavity also needs to be fed by some sort of transmission line. Considering the geometry of the antenna and the desired frequency band, a conventional WR90 waveguide was chosen (Fig. 3.2) [1].

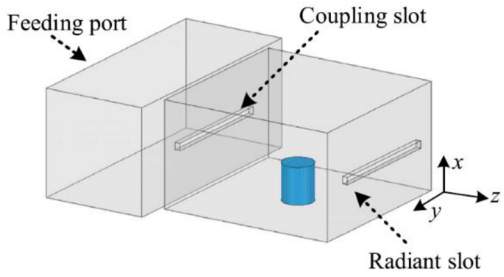

Fig. 3.2 First -order coaxial cavity filtering antenna using slot coupling [1]

This configuration's drawback is that altering the length of the resonating cylinder will not only change the resonant frequency but also lower the quality factor, which will decrease the antenna's effectiveness. Slots were swapped out for a pair of cylinders to solve this issue (Figure 3.3). First one acts as a coupling slot and the second acts as a radiation slot. By varying their length together with the cylinder responsible for tuning frequency, we ensure that there is no loss of quality factor over the entire frequency range of the antenna.

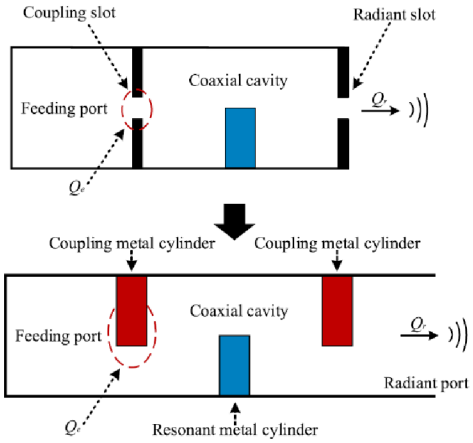

Fig. 3.3 Evolution process of the novel coaxial filtering antenna structure [1]

3.2 First order filtering waveguide antenna

Table 3.1 Length of resonant cylinders for frequency tuning

Frequency tuning						
Frequency [GHz]		lr [mm]	h [mm]		lr [mm]	h [mm]
9,25		8,81	6,56		8,80	6,53
9,50		8,63	6,36		8,63	6,36
9,75	Original	8,52	6,12	HFSS	8,39	6,15
10,00		8,43	5,88		8,45	5,89
10,25		8,32	5,65		8,20	5,67
10,50		8,11	5,45		8,13	5,46
10,75		7,95	5,23		7,96	5,24

Table 3.2 Length of resonant cylinders for frequency tuning

Bandwidth tuning							
Bandwidth [MHz]		lr [mm]	h [mm]		lr [mm]	h [mm]	Bandwidth [MHz]
50		8,43	5,88		8,35	5,92	60
100	Original	7,77	6,15	HFSS	7,76	6,15	110
150		7,30	6,37		7,35	6,33	148
200		6,98	6,58		7,07	6,45	202

Antenna from the research paper was modelled in the HFSS electromagnetic simulator according to the template [1] because the primary goal of the semester project is to confirm the functionality of the presented antenna. An aluminium block that is hollow makes up the antenna's initial design. Internal cross section dimensions (a = 22.86 mm, b = 10.16mm) are those of a typical WR90 waveguide.

Three cylinders with a diameter of 3 mm are than positioned in the middle of the waveguide (Fig. 3.4) in the direction of the Z-axis to provide function of frequency and quality factor tuning.

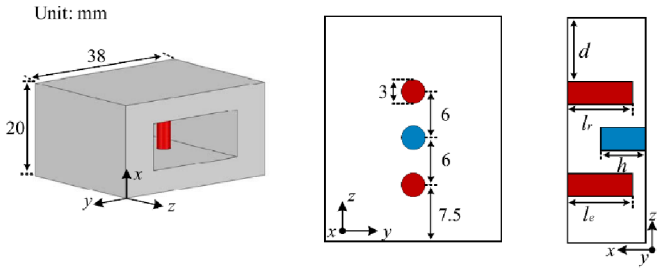

Fig. 3.4 Geometry parameters of the first-order coaxial filtering antenna[1]

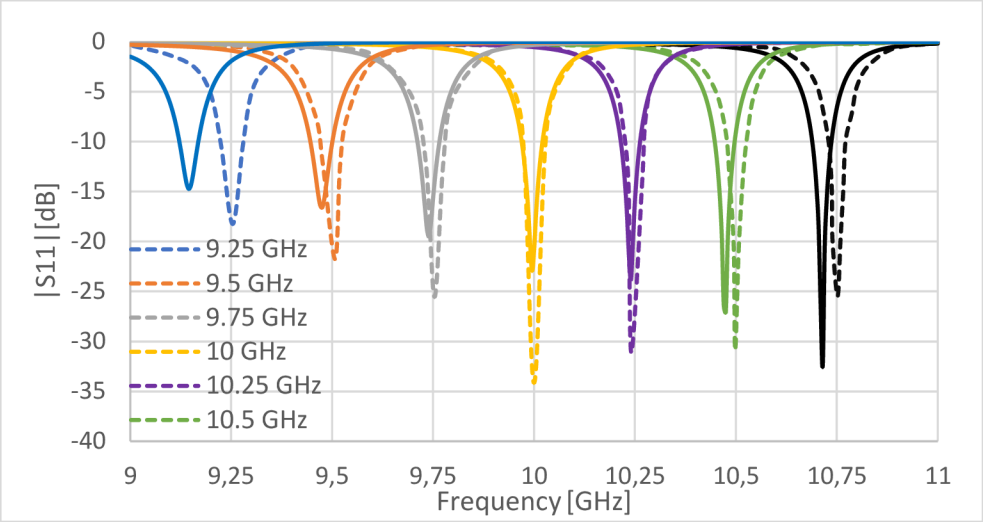

Fig. 3.5 S11 of the first-order filtering antenna with tuneable frequency simulated (full line), article (dashed line) [1]

Two operating modes are possible for the proposed antenna. The first one is independent tuning of operating frequency, in which the antenna's resonant frequency can be continuously adjusted between 9 and 11 GHz using tuning pins, while the bandwidth is held constant and is capped at about 50 MHz (Fig. 3.5) Second mode of the antenna allows tuning the bandwidth without changing the resonant frequency, at the cost of a lower value of the reflection coefficient S11. A demonstration of this function is shown in (Fig. 3.7)

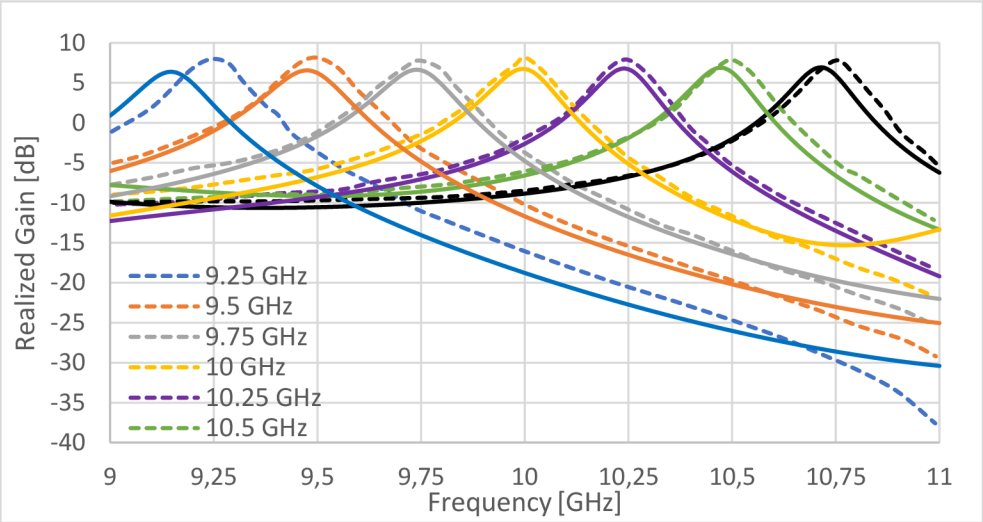

Fig. 3.6 Simulated Gain of the first-order antenna with tuneable frequency simulated (full line), article (dashed line) [1]

As we can see from the simulated figures obtained from HFSS values differ from those reported in paper [1]. In the simulation of the S-parameters, larger deviations occur with increasing distance from the centre frequency of 10 GHz, for which the waveguide is primarily designed. Due to the optimal impedance matching, antenna obtains lowest reflection coefficient at this frequency. These differences are primarily caused by different simulation settings as well as computational accuracy, since the paper does not specify anywhere under what circumstances the model was simulated. Despite the highest possible accuracy used, which computer was able to achieve, there are minor discrepancies in simulated results. Nevertheless, both tuning functionalities of antenna are maintained.

At the beginning of simulation, depth of pins was set according to research paper (Table 3.1) [1] Figure (3.)5 shows comparison of the reflection coefficient between the values within the article [1] and the values obtained by me with limited precision. Reduced accuracy had only a minimal effect on the frequency shift of antenna resonant frequencies, in most cases there was a shift of less than 20 MHz and an average decrease in value of reflection coefficient by 10 dB. Table (3.1, 3.2) shows a comparison of the pin length that we would need to set to match the results reported in the paper. Changes that would have to be made in order to obtain same result are no more than tenth of a millimetre. Therefore, we can conclude that the discrepancies in graphs are only due to lower computational precision.

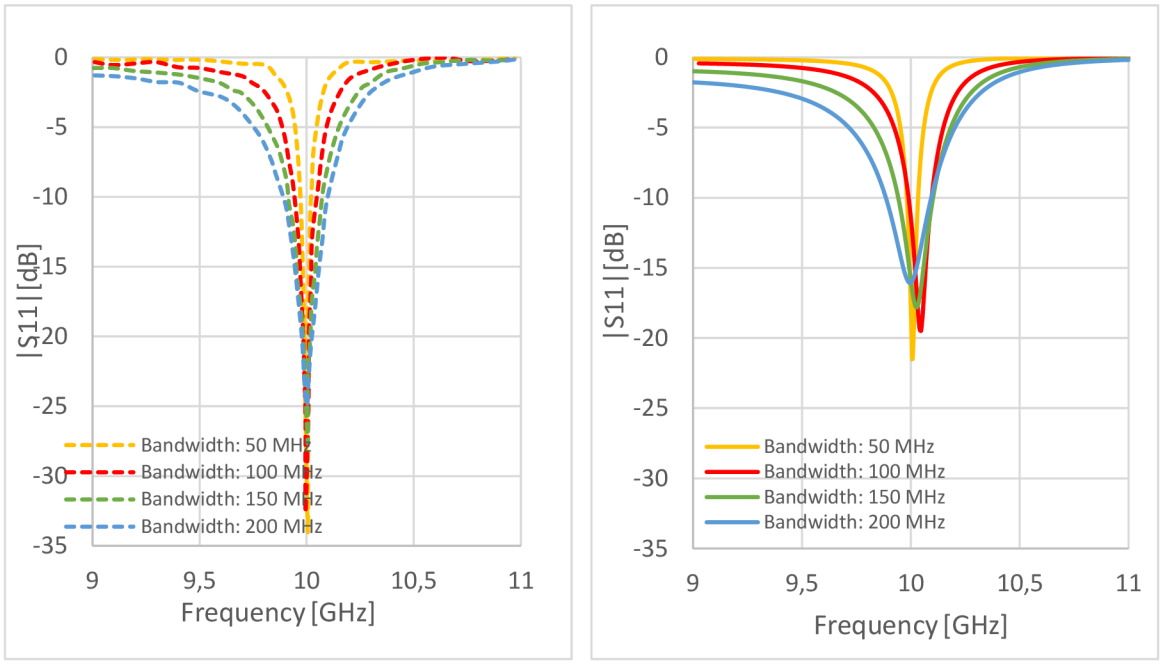

Fig. 3.7 Simulated results of the first-order antenna with tuneable bandwidth

b) simulated (full line) a) article (dashed line)

Simulated antenna achieves a directivity of 7.7 dB and its main lobe is parallel to the antenna's z-axis (Fig. 3.9). When tuned to the resonant frequency, gain remains constant, reaching maximum of 7.5 dBi (Fig. 3.6), compared to the value of 8.1 dBi reported in the research paper [1]. Therefore, simulations confirmed correct functionality of proposed antenna concept.

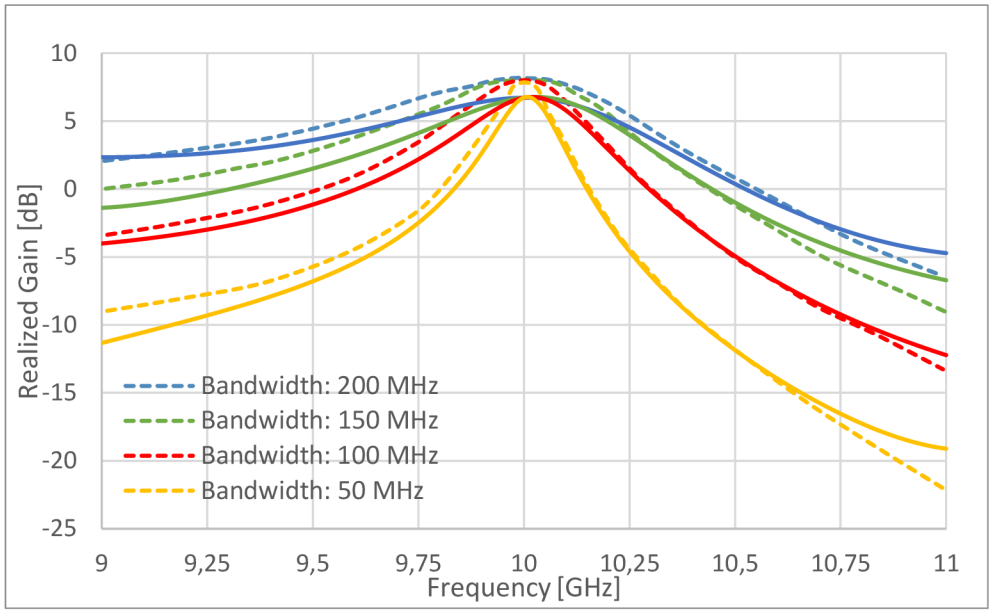

Fig. 3.8 Simulated Gain of the first-order antenna with tunable bandwidth simulated (full line), article (dashed line) [1]

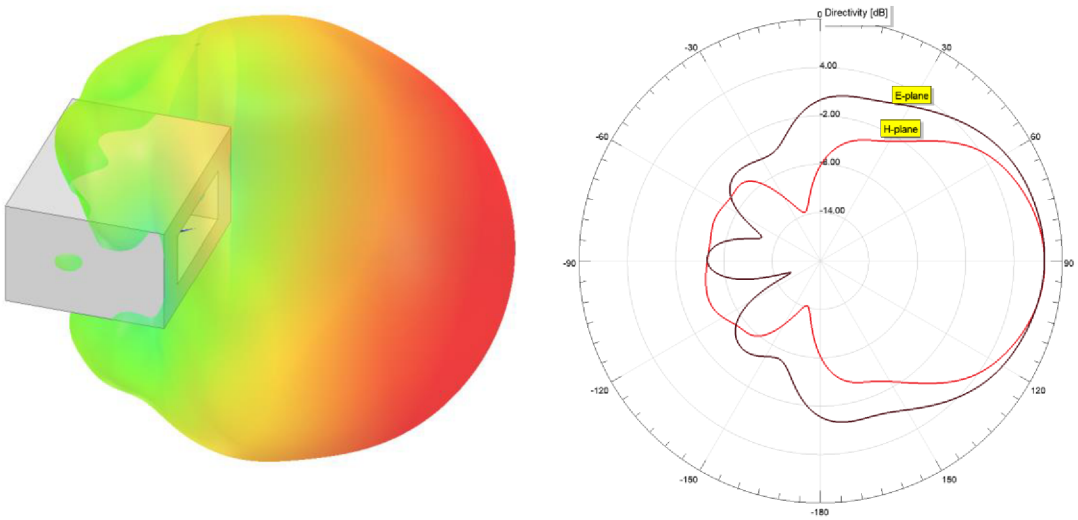

a) b)

Fig. 3.9 Directivity pattern of an first order filtering antenna a) 3D-diagram b) directivity in E-plane, H-plane

4. IMPROVING PARAMETERS OF PROPOSED ANTENNA

One of the disadvantages of antenna proposed in Chapter 3 is that the antenna selectivity decreases with increasing bandwidth. Selectivity is an important parameter in antenna design so that it can receive the wanted signal at the wanted frequency and attenuate unwanted signals. Selectivity of the receiver determines level of signal interference that is commonly found in free space. It is very important that the selectivity allows sufficient suppression of the signal at out-of-band frequencies. If two signals are present on the same channel, receiver selectivity cannot distinguish between them. By increasing the selectivity of the antenna, we increase the utilisation of the allocated frequency band. Therefore, an antenna with a third order filter is proposed in [1].

4.1 Third-order filtering antenna

To improve antenna selectivity, a third-order filtering antenna is proposed in [1]. This is an iteration of the antenna from the previous chapter (3.2). Consisting of an extended WR90 waveguide with geometry displayed in (Fig. 4.1). Additional tuning pins were also inserted into the cavity. On the bottom side there are 3 tuning screws which provide tuning of the resonant frequency thereby forming a third order filter. At the top are placed 4 pins which again affect the coupling between each cylinder. Pins *l2* sets quality factor of radiating (*Qr*) and feeding port (*Qe*) while pins *l1* provides coupling between three resonant cylinders.

We can say that the third-order filtering antenna retains same characteristics as the first-order filtering antenna. The function of independent tuning of resonant frequency and bandwidth is retained. Due to the increase in the number of resonant pins, the minimum tunable bandwidth has increased to 200 MHz. Gain is uniform across the tuned bandwidth and reaches 8.1 dBi. When using a third-order filtering antenna, there is an improvement in selectivity and suppression of unwanted signals of more than 70 dB over conventionally used slot antennas [1].

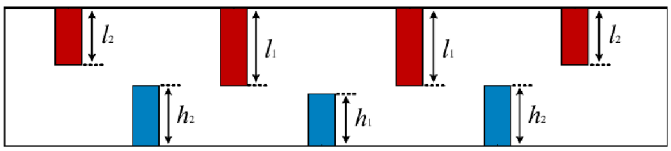

Fig. 4.1 Schematics of third-order filtering antenna[1]

4.2 Horn antenna

By flaring out standard waveguide we get a horn antenna with an open end. This is widely used type of antenna for the UHF and microwave bands. Since the resonant frequency depends on the physical dimensions of antenna, this type of antenna is used only for frequencies higher than 300 MHz. The main advantage is their simple construction, moderate directivity as well as weather resistance. Function of the flaring at the waveguide end is to produce a uniform wave that is larger than the wave being propagated inside the waveguide. There are several basic types of horn antennas, with a rectangular cross-section (Fig. 4.2c), a circular cross-section (Fig. 4.2 d), or antennas with flaring in only one of the planes, E-plane (Fig. 4.2 b), H-plane (Fig. 4.2 a).

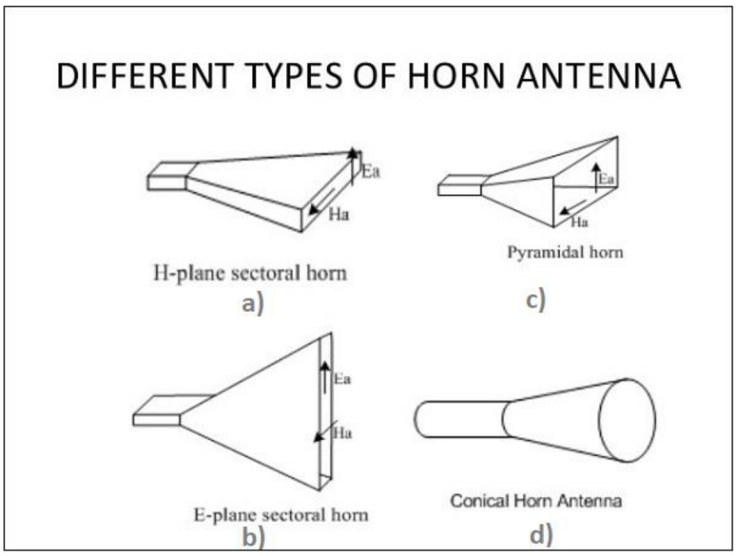

Fig. 4.2 Different types of horn antenna [5]

We can change the resonance frequency and bandwidth by utilizing the antenna from chapter (4.1). Third-order filtering antenna's limited directivity and low gain might not be adequate for some applications. However, by adjusting the tuning pins, we are unable to change these parameters. The subsequent chapters suggest modifying the antenna to enhance directivity and gain.

4.3 Improving parameter of third-order filtering antenna

The aim of this subsection is to verify whether it is possible to improve the parameters of proposed antenna [1]. Since third-order filtering antenna designed in this way achieves a small gain of 8.1dBi and the main lobe has a width of 63°, which is an insufficient value for use in applications such as radar and radio communications.

To improve these parameters, we could add a horn antenna to the end of the waveguide and verify its unchanged filtering functionality. If the filtering characteristics of waveguide were unchanged, this would mean that we could add any horn antenna with the desired gain and directivity to the third-order filtering antenna.

The basis of improved antenna design is third-order waveguide antenna, performance of which was verified in Chapters 2 and 3. One of the antennas from subsection (4.2) can be placed at the end of the waveguide. Since in this case the cross-section of the waveguide is rectangular, we will not consider a horn antenna with conical shape. Its integration is possible but would require an additional design of a transformer from a rectangular to a circular interface. For demonstrative purposes, we will use a pyramidal antenna. Model of the antenna was created in CST Microwave studio, based on 3D drawings provided by the manufacturer (chapter 4.3.1) [6].

Shape of the antenna itself consists of two parts, namely the original rectangular third-order filtering antenna and the horn antenna added by us. Detail of the whole geometry is shown in (Fig 4.3). The addition of the horn antenna has increased total length of structure to 148 mm, from 68 mm, which is more than double the size of proposed antenna. If the use of the antenna is limited by the dimensions, we can use shorter type of horn antenna, as they are produced in different designs.

The last modification made was to standardize the wall thickness of the waveguide and horn antenna to 2.1 mm. Original design foresees wall thicknesses of 7,57 mm and 4,92 mm. However, these values are unusually high for a WR90 waveguide, compared to the values given by the standards. It has been verified through simulation that the wall thickness does not affect the observed antenna parameters.

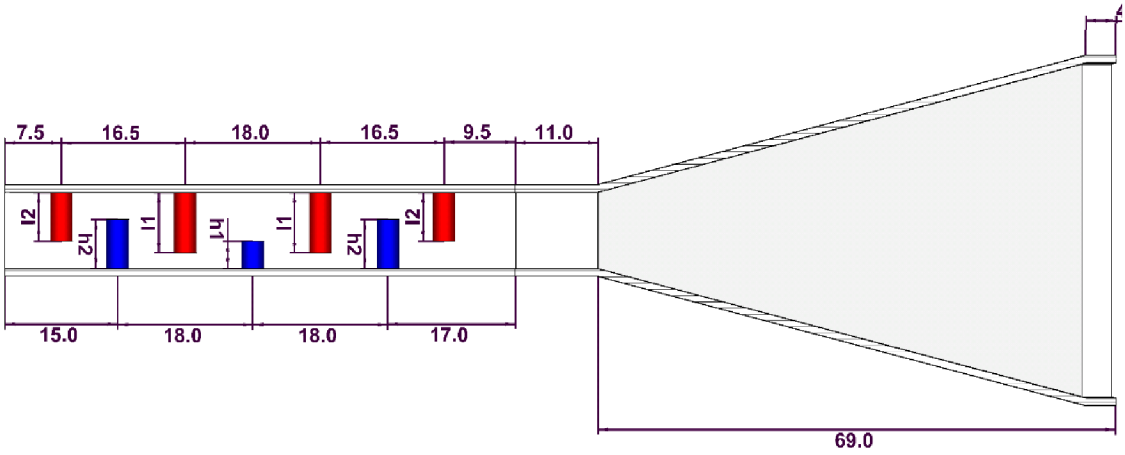

Fig. 4.3 Dimension of filtering waveguide horn antenna

4.3.1 Commercially available horn antenna

There are many types of commercially available horn antennas on the market with different parameters. For demonstrative use, a pyramidal antenna [6] from the manufacturer PASTERNACK was chosen, used for frequencies from 8.2 to 12.4 GHz and declared gain of 15 dBi. It is an antenna based on a WR90 waveguide, which is fed by a coaxial N connector. Antenna aperture dimensions are a = 62 mm, b = 44,6 mm.
A 3D model of the antenna is also available from the manufacturer's website (Fig. 4.4) This information's has been used to model antenna for the simulation in CST Microwave studio.

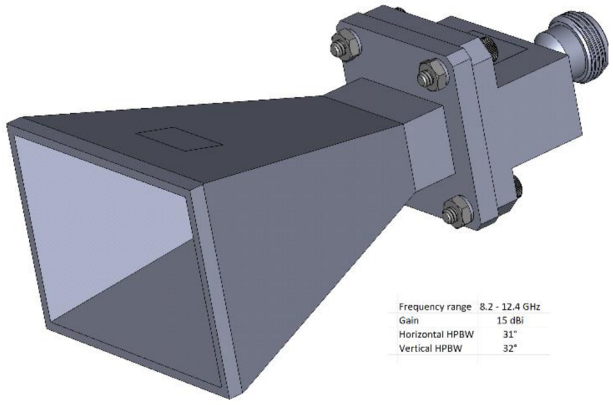

Fig. 4.4 Commercial Horn antenna [6]

4.3.2 Simulation settings

Whole designed antenna was simulated in CST Microwave Studio 2020. Figure (4.5) shows how the feeding coaxial N connector was added to the modified antenna model. Its outer conductor is connected to the body of the waveguide and a coaxial probe is inserted into the cavity.

To reduce the computational time, a half-size model was made, thanks to longitudinal symmetry of the antenna. Results between the half-model and the full-model showed no differences and thus we could save almost half of the computation time. We used freed memory space to refine meshing of the half model to obtained even more accurate results.
-

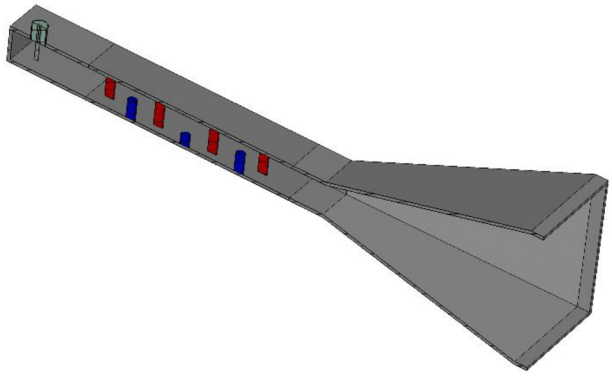

Fig. 4.5 Half model of deigned antenna with coaxial N connector

4.4 Obtained results of improved antenna

This chapter focuses on the comparison between the results of proposed third-order filtering antenna [1] and the filter antenna where the opened end is replaced by a horn antenna. In order to ensure as accurate comparison as possible, the same pin length was used for both antennas. Length of the individual pins for resonant frequency tuning and bandwidth tuning are shown in the tables (Table 4.1 and Table 4.2)

-

Table 4.1 Cylinder dimensions during frequency tuning

Frequency tuning				
Frequency [GHz]	l1[mm]	l2 [mm]	h1[mm]	h1[mm]
9.25	9.28	7.70	4.28	5.17
9.5	9.17	7.57	3.96	4.90
9.75	9.02	7.36	3.62	4.64
10	8.82	7.16	3.26	4.38
10.25	8.60	6.92	2.84	4.12
10.5	8.35	6.70	2.33	3.86
10.75	8.04	6.51	1.64	3.56

Table 4.2 Cylinder dimensions during bandwidth tuning

Bandwidth tuning				
FBW	l1 [mm]	l2 [mm]	h1[mm]	h1[mm]
2%	8.82	7.16	3.26	4.38
4%	8.20	6.56	3.51	4.63
6%	7.55	6.20	3.79	4.82
8%	6.93	5.89	4.10	5.00

Comparing simulated values of the S_{11} parameters we found, that adding the horn antenna to the end of the waveguide does not shift tuned resonant frequencies. However, horn slightly degrades impedance matching of the whole array. Consequence of this is that, when tuning frequency bands in the 9.5 GHz to 10 GHz range, the reflection coefficient does not reach values <-10 dB across the whole tuned range. Bandwidth, therefore, drops to 150 MHz. This is mainly because the added horn antenna affects quality factor *Qr* of the radiation port, which can be seen from the plot (Fig. 4.6), where the characteristic has an asymmetric shape. This behaviour can be partially eliminated by tuning the pin placed closest to the horn antenna. By this adjustment we can back-tuned antenna so that bandwidth reaches 200 MHz over the whole frequency range. However, the *l1* pins will no longer be the same length, which slightly complicates the antenna tuning process.

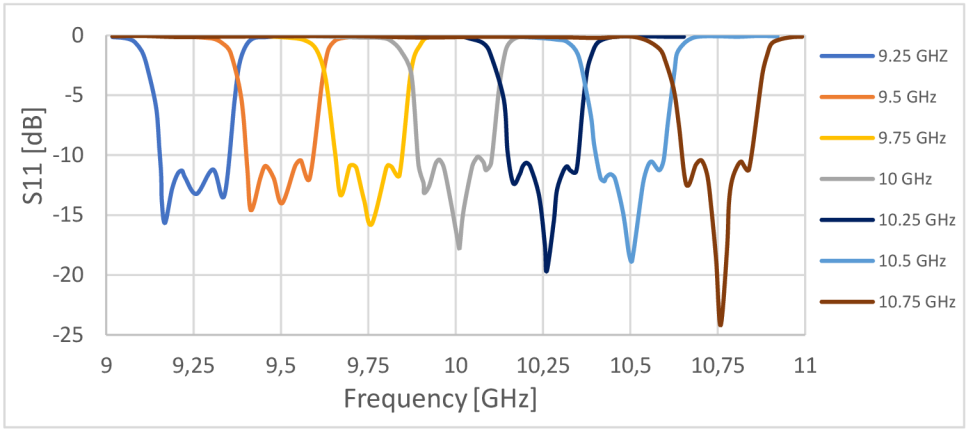

a)

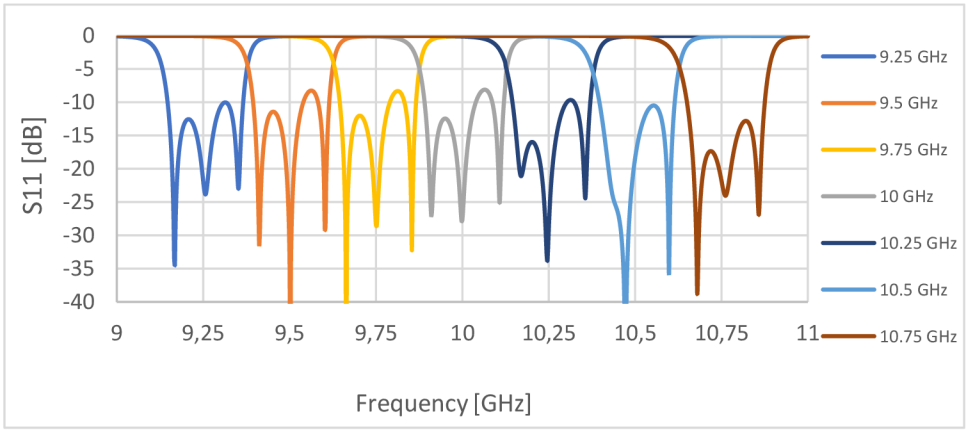

b)

Fig. 4.6 Reflection coefficient S11 comparison between a) 3rd-order filtering antenna [1], b) 3rd-order filtering horn antenna while performing frequency tuning [1]

Gain of the antenna assembly is uniform over the entire tuned range (Fig 4.7). When the horn antenna was added to the end of filtering waveguide, gain rose to 14.9 dBi (Fig 4.7), which is very close to the manufacturer's declared value of 15 dBi [6]. Since the addition of the horn antenna does not substantially changes function of the original 3rd-order filtering antenna, we can swap the horn antenna for another desired type if higher gain or directivity is needed. The disadvantage of the filtering horn antenna is that selectivity has decreased, across all frequency bands.

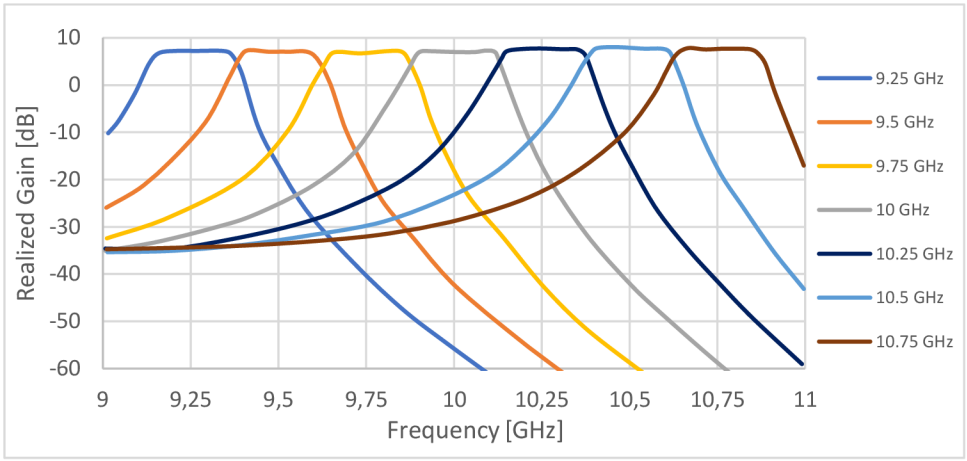

a)

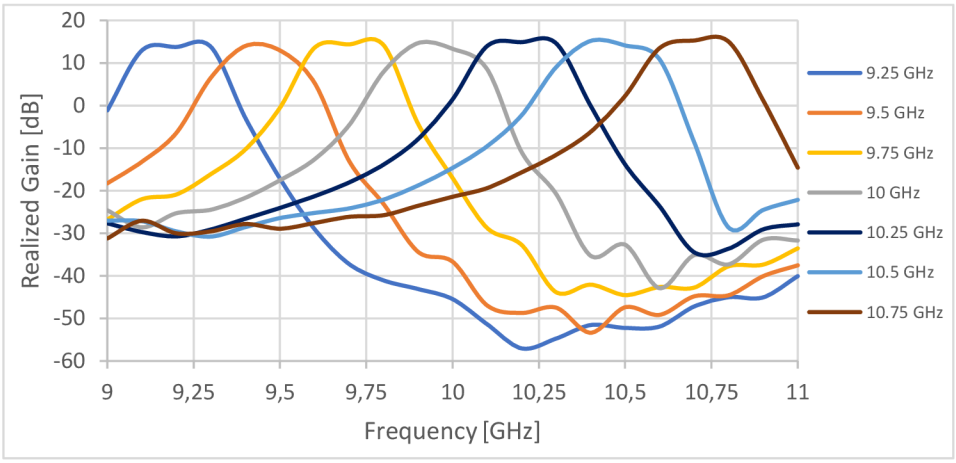

b)

Fig. 4.7 Gain comparison between a) 3rd-order filtering antenna [1], b) 3rd-order filtering horn antenna while performing frequency tuning

The function where the bandwidth can be tuned independently has also been retained. In (Fig 4.8 (b)) we can observe same asymmetry as in the resonant frequency tuning mode (Fig 4.6 (b)). Reflection coefficient S_{11} again does not reach <-10dB across the tuned band, reducing our usable bandwidth. This behaviour can again be compensated for by

slightly tuning coupling pin 11. Figure (4.9) shows that even when using antenna in the bandwidth tuning mode, gain remains stable with a maximum of 14.9 dBi.

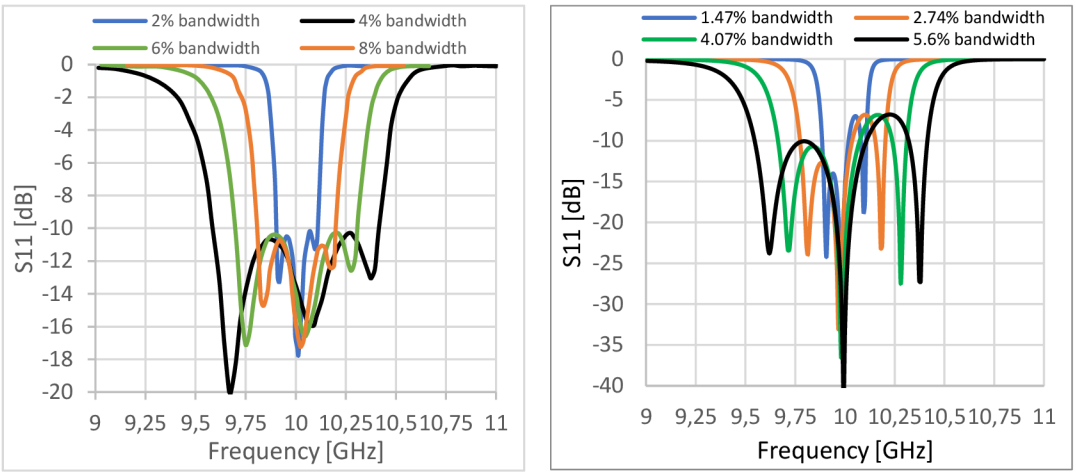

a) b)

Fig. 4.8 Reflection coefficient S11 comparison between a) 3rd-order filtering antenna [1], b) 3rd-order filtering horn antenna while performing bandwidth tuning

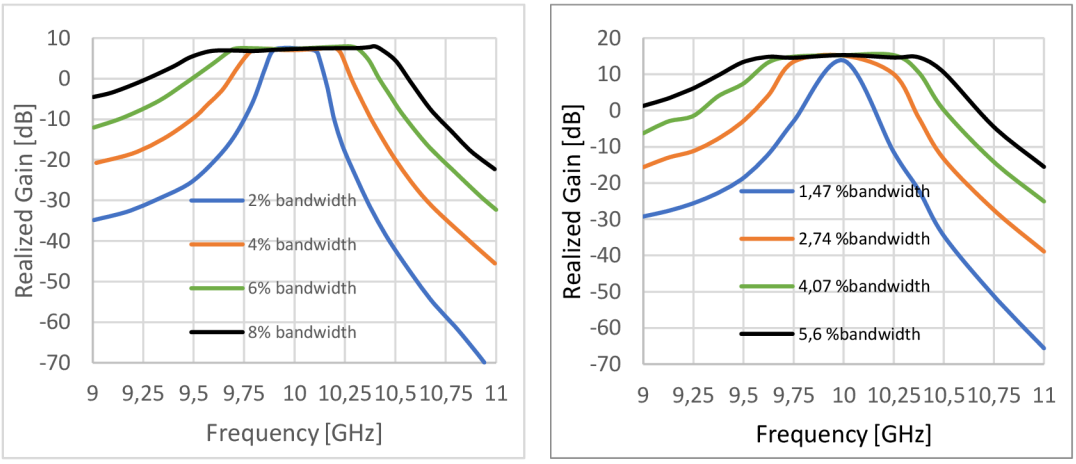

a) b)

Fig. 4.9 Gain comparison between a) 3rd-order filtering antenna [1], b) 3rd-order filtering horn antenna while performing bandwidth tuning

Directional gain characteristics are shown in (Fig. 4.10). Main lobe of the diagram points in line with the antenna z-axis Theta = 0° and reaches 14.9 dBi. Half power beam width (HPBW) reaches 34° in the H-plane and 32° in the E-plane, which are half of the values compared to a 3-rd order filtering antenna [1]. Side lobes are suppressed by more than -17 dB in both planes. As demonstrated earlier in this chapter by changing the

geometry of the horn antenna we can also achieve higher values of directivity and gain depending on the desired antenna characteristics.

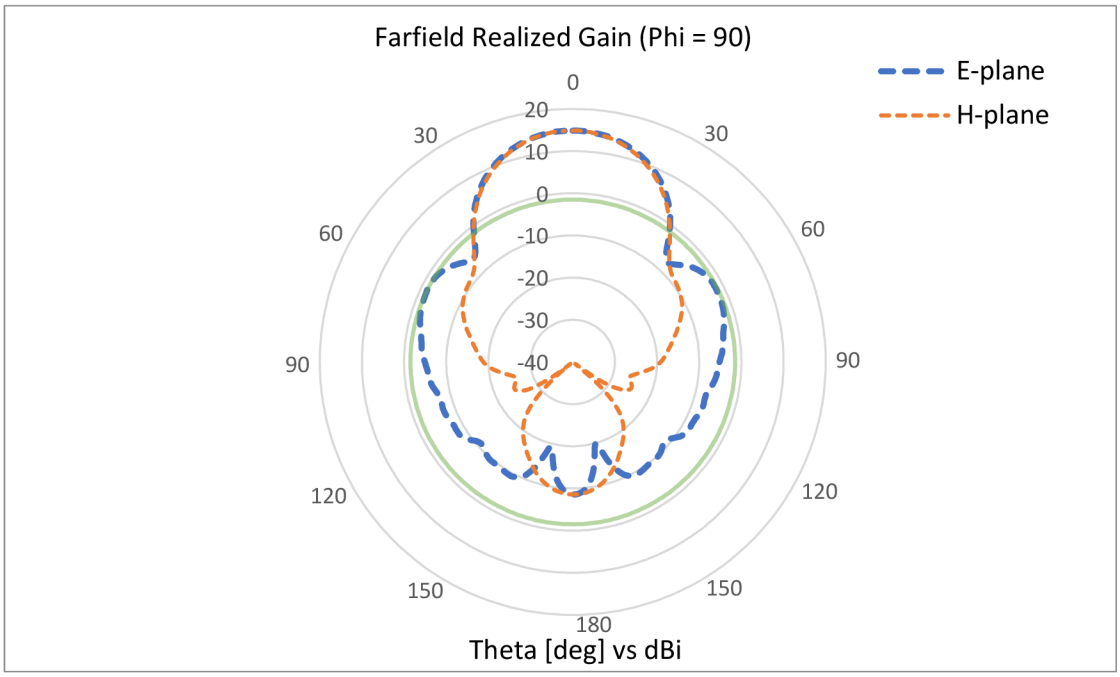

Fig. 4.10 Directional gain pattern of improved antenna

5. SUBSTRATE INTEGRATED WAVEGUIDE ANTENNA

The next chapter focuses on the design and optimization of a tuneable substrate integrated antenna (SIW) for use in the European standard for High Performance Wireless Local Area Network (HIPERLAN). Proposed antenna can be tuned in the HIPERLAN frequency range spanning from 17.1 to 17.3 GHz. The study also aims to validate the feasibility of modifying the cavity-based waveguide antenna described in the previous chapters into a tuneable antenna integrated into the substrate.

5.1 Substrate integrated waveguide

SIW are closely related to rectangular waveguides. In both types of waveguides, same principles of wave propagation apply. Difference in the construction of SIW is its tapering in the E plane. The basis of the SIW is a block of substrate with defined permittivity coated with thin layer of metal on both sides. Permittivity of chosen substrate significantly affects passband of the SIW and has an effect on the resulting wavelength. With increasing substrate thickness bandwidth also increases. For the construction of a reliable waveguide, we must also take into consideration important parameters such as, constant permittivity in the entire used frequency range, small loss factor, as well as the frequency and temperature stability of the substrate.

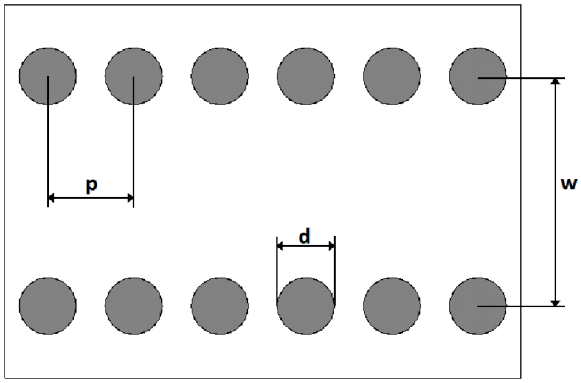

Fig. 5.1 Main dimensions of SIW

In contrast to the cavity waveguide, plating the side walls of the SIW is not a viable option. Therefore, plated side walls are replaced by periodically repeating vias (Fig. 5.1) at p with a diameter d which connects the lower and upper metal layers of the waveguide. Incorrectly designed gaps between the vias may cause radiation leakage, which is not an issue with a hollow waveguides. To minimize waveguide losses, vias must fulfil two basic qualitative conditions [11]. The diameter of the vias d should not exceed fifth of the wavelength λg that propagates through the waveguide.

$$d < \frac{\lambda_g}{5} \tag{5.1}$$

Distance p between individual vias should not exceed twice the diameter of the via.

$$p < 2d \tag{5.2}$$

By satisfying these conditions (Equation 5.1 and 5.2), we ensure minimum signal transmission losses as well as reduction in waveguide fabrication complexity.

5.2 Wave propagation inside SIW

Substrate-integrated waveguides and cavity waveguides have comparable propagation characteristics of electromagnetic energy. In a cavity-based waveguide, the conditions for the formation of infinite number of TE and TM modes are met. If we try to excite wave in the waveguide whose currents flow perpendicular to the opening there would be significant radiation outside the waveguide through spaces between the vias and a significant attenuation of the electromagnetic wave. Due to discontinuities in the walls of the waveguide formed by the vias, SIW is unable to maintain these modes, therefore only modes TEn0 can propagate through the SIW [12]

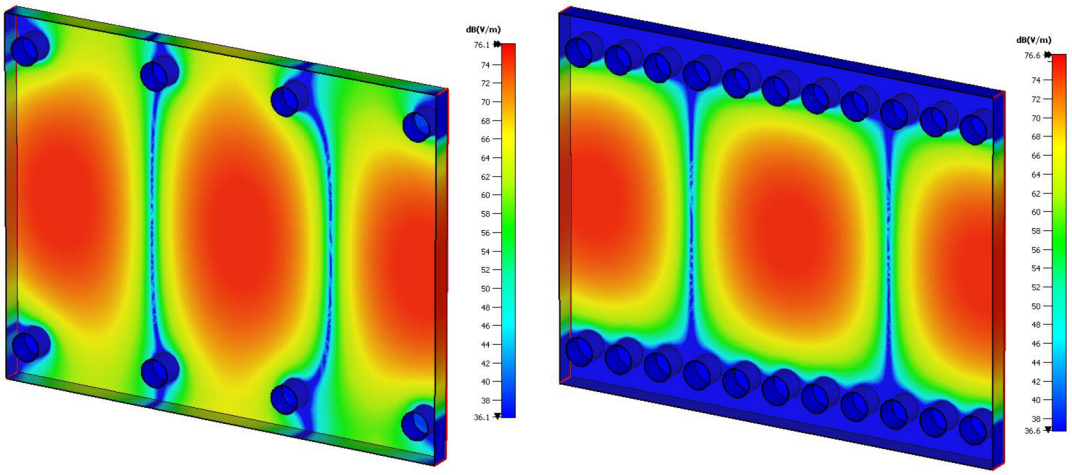

a) b)

Fig. 5.2 Wave propagation in SIW with incorrect vias spacing a) 5mm and correct vias spacing b) 1.5mm

As mentioned, leakage losses can be controlled by proper design of the vias. Figure (5.2) demonstrates the excitation of the TE_{10} mode for different parameters of the vias. Simulation was performed at 17 GHz where all metallic surfaces were replaced by an ideal electric conductor (PEC).

For both cases the waveguide is made of CuClad217 substrate with relative primitivity e_r = 2.17 and dielectric constant δ = 0.0009. Figure (5.2 a) demonstrates the case when the vias with diameter d = 2mm are placed at 5mm in this case they are placed too far apart and do not satisfy the condition (Equation 5.2) resulting in a significant radiation through the gaps between the vias.

From the second figure (5.2 b) we can see by placing vias at a distance p = 1.5 mm the electromagnetic energy in the H-plane passes to the end of the waveguide with minimal losses. The diameter of the via does not have a significant effect on the wave propagation as long as it satisfies the condition (Equation 5.1).

5.3 Design of SIW for 17 GHz

5.3.1 Choice of material

The choice of substrate can influence not only the electrical but also the mechanical properties of the waveguide integrated into the substrate. CuClad217 material was chosen because of its low permittivity and easy availability in UREL workshops. Parameters of the substrate used can be seen in Table (5.1), the values were taken from the datasheet provided by manufacturer [13].

Table 5.1 Parameters of substrate CuClad 217

Substrate	ε_r [-]	tan δ [-]	Height [mm]	Cladding thickness[μm]
CuClad217	2.17	0,0009	1.52	17.5

5.3.2 Design of SIW

SIW waveguide design is based on exploiting similarity with the cavity waveguide. Transformation between waveguides is shown in the Figure (5.3) where a and b indicate the width and height of the rectangular waveguide, respectively. By changing these two parameters, we can adapt the waveguide to transmit a signal of any frequency see Chapter 1. For a waveguide integrated into a substrate, we are unable to control its height as this is determined by the thickness of the substrate. Therefore, SIW waveguides are tuned using the diameter of the vias d distance between the vias p and the width of the waveguide w (Fig. 5.1)

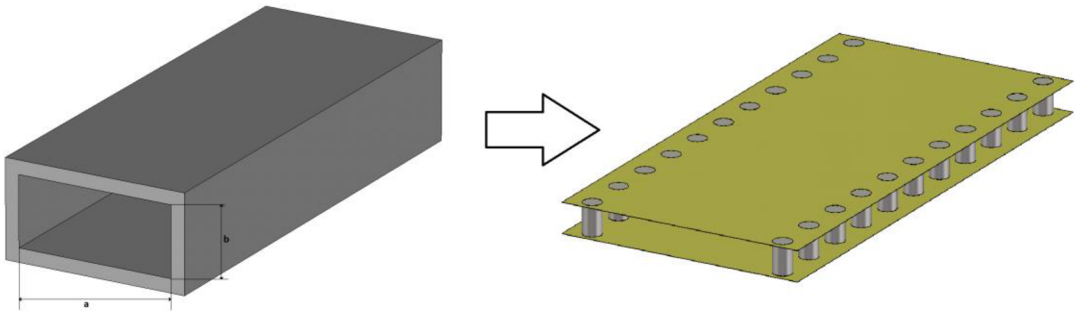

Fig. 5.3 Transformation of rectangular to SIW waveguide

Designed waveguide should be capable of transmitting electromagnetic energy at a frequency 17 GHz with minimal losses. Operating frequency is chosen to be sufficiently far from the cutoff frequency of the SIW to avoid attenuation in the transmission of the signal. Modelling of the waveguide is initiated by calculating critical frequency for waveguide [14]:

$$f_c = \frac{c}{2\pi\sqrt{\epsilon_r}} \times \sqrt{\left(\frac{m\pi}{w}\right)^2 + \left(\frac{n\pi}{h}\right)^2} \tag{5.3}$$

Where *m* represents the number of half waves of electromagnetic field along the wall *w* in waveguide with a rectangular cross-section. Mode number *n* defines the number of half-waves alongside wall *h*. Constants **c** defines speed of light and ε_r defines the permittivity of a substrate through which electromagnetic wave propagates. From this expression we can then derive dependency for the wavelength [14]:

$$\lambda_c = \frac{2\pi}{\sqrt{\left(\frac{m\pi}{w}\right)^2 + \left(\frac{n\pi}{h}\right)^2}} \tag{5.4}$$

Waveguide is designed in such a way that only the transverse electric wave TE_{10} propagates through it. Previous relations can therefore be modified to the form:

$$f_c = \frac{c}{2\pi\sqrt{\epsilon_r}} \times \sqrt{\left(\frac{m\pi}{w}\right)^2} \tag{5.5}$$

$$\lambda_c = 2w \tag{5.6}$$

Equations (5.5 and 5.6) show that the cutoff frequency of the waveguide depends on the relative permittivity of substrate and spacing of two rows of vias. Since the wave propagates through the substrate in the SIW, we have to consider the shortening of the wavelength [14]:

$$\lambda_g = \frac{\lambda}{\sqrt{1 - \left(\frac{\lambda}{\lambda_c}\right)^2}} \tag{5.7}$$

Where λ represents the wavelength in vacuum and λc the cutoff frequency of the waveguide. If the conditions (Equation 5.1 - 5.2) are satisfied and the cutoff frequency is known, we can select the parameters of the vias prior to the optimization in the electromagnetic simulator according to (Fig. 5.4).

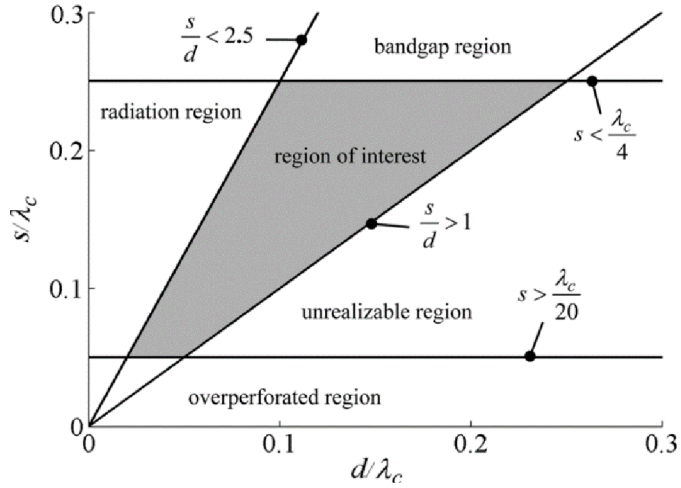

Fig. 5.4 Recommended dimensions of vias [17]

5.3.3 Design of SIW in electromagnetic simulator

Figure (5.5) displays SIW model that was simulated in CST microwave studio. Initially waveguide width w=10mm was based on equation (5.4) used for determining critical frequency of waveguide. Diameter and spacing of the vias were chosen so they satisfy the conditions (Equation 5.1 - 5.2) and recommendations for SIW waveguide design (Fig. 5.4). Diameter of the via p = 1mm was chosen with future antenna fabrication in mind so that vias could be drilled with a standard set of metric drill bits. Spacing of the vias d = 2mm ensure minimal losses and ensures mechanical strength of the SIW

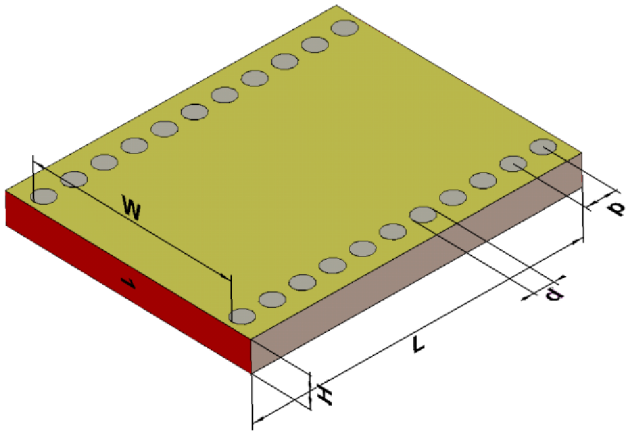

Fig. 5.5 Model of substrate integrated waveguide

-

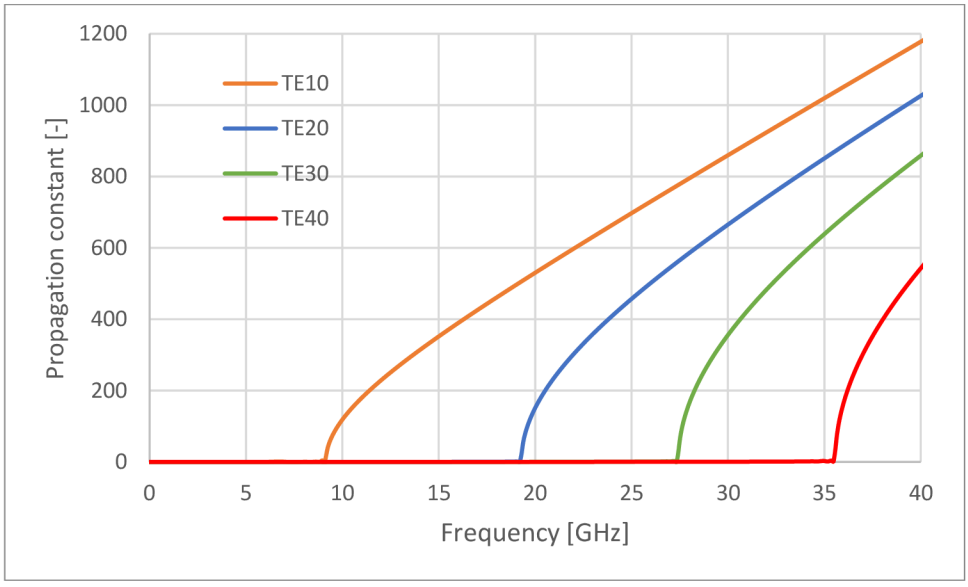

Fig. 5.6 Cut-off frequencies for different modes in proposed SIW

SIW model (Fig. 5.5) consists of a CuClad 217 substrate with permittivity $\varepsilon_r = 2.7$. Both sides of the waveguide were coated with 17.5 µm thick copper layer. Vias were symmetrically spaced at a distance W/2 from the centre of the waveguide and connected to the top and bottom conductive layers of the waveguide. To increase its mechanical strength, the substrate has been widened by 3 mm on both sides pass the vias. Table (5.2) shows all the dimensions of proposed waveguide.

Table 5.2 Dimensions of simulated waveguide

p [mm]	W[mm]	H [mm]	L [mm]	d [mm]
1.5	10	1.52	16.5	1

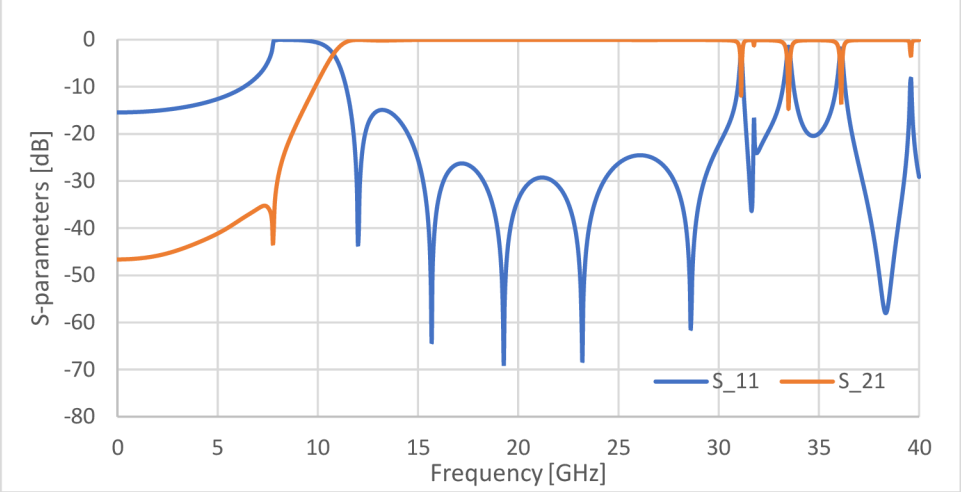

Fig. 5.7 Reflection and Transmission coefficients of simulated SIW

Overall waveguide length L has no effect on the waveguide performance in the simulation. To minimize the simulation time, the length was adjusted to double the wavelength λ_g. Figure (5.7) shows the characteristic of the reflection coefficient S_{11} of the dominant mode TE_{10}, which reaches – 68 dB at 17 GHz. And the transmission coefficient S_{21} is approaching a value very close to 0 dB. Next higher mode TE_{20} starts to become dominant only above the frequency of 20 GHz. Usable bandwidth of the single mode waveguide reaches 15 GHz in this region, the reflection coefficient is below – 20dB and the transmission coefficient of S_{21} is higher than -2dB indicating high efficiency of the proposed waveguide.

Through optimization in CST, the SIW waveguide width was tuned to width of10.5 mm so that the operating frequency of the waveguide corresponds to approximately 1.4 times the critical frequency. Table (5.3) clearly shows the achieved parameters of the designed waveguide. By adjusting the distance **w** between the vias, it is possible to change the operating bandwidth of the waveguide in a wide frequency range.

Table 5.3 S-parameters of SIW at 17 GHz

	S1,1 [dB]	**S2,1 [dB]**	**VSWR**
SIW (w=10,5mm)	-69,08	-0,046	1,001

5.4 Feeding substrate integrated waveguide

To generate an electromagnetic field in a waveguide integrated into the substrate, three basic methods of feeding are used. The first two methods utilize microstrip and coplanar lines where microstrip line perform the job of quarter wave transformer and match the impedance level on both ends of transmission line. The third feeding method using coaxial lines is described in more detail in the next subsection.

5.4.1 Coaxial to SIW transition

Feeding SIW through a coaxial probe is a widely used technique, mainly due to the low parasitic radiation of coaxial cable compared with microstrip transmission lines. This parasitic radiation causes distortion of the radiation pattern and reduces the overall efficiency of the waveguide. Another reason to use a coaxial probe is to maintain bandwidth up to 20%. Another advantage is that it is easily integrated into the waveguide, which reduces production costs.

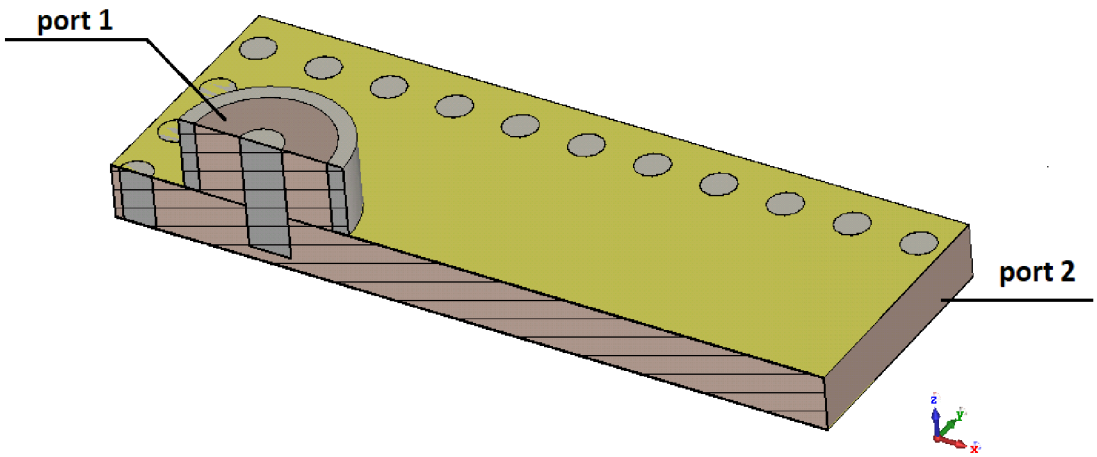

Fig. 5.8 Feeding SIW via coaxial cable

Design rules for feeding SIW are same as for feeding rectangular waveguide from chapter 1. Due to the low thickness of the substrate, on the order of only a few millimetres, it is difficult to accurately set the depth of the coaxial probe. This problem is described in [15] where the problem is solved in a way where the outer conductor of the coaxial probe is conductively connected to the upper metallic layer of the substrate. The inner conductor of the coaxial probe is then passed through the substrate and conductively connected to the bottom metal layer of the waveguide. However, a coaxial probe connected in this manner has an adverse effect on the bandwidth of the waveguide. Figure (5.8) shows an alternative waveguide feed solution where only the outer conductor of the waveguide is connected to the metallic surface and the inner conductor is left hanging freely in a hole drilled into the substrate.

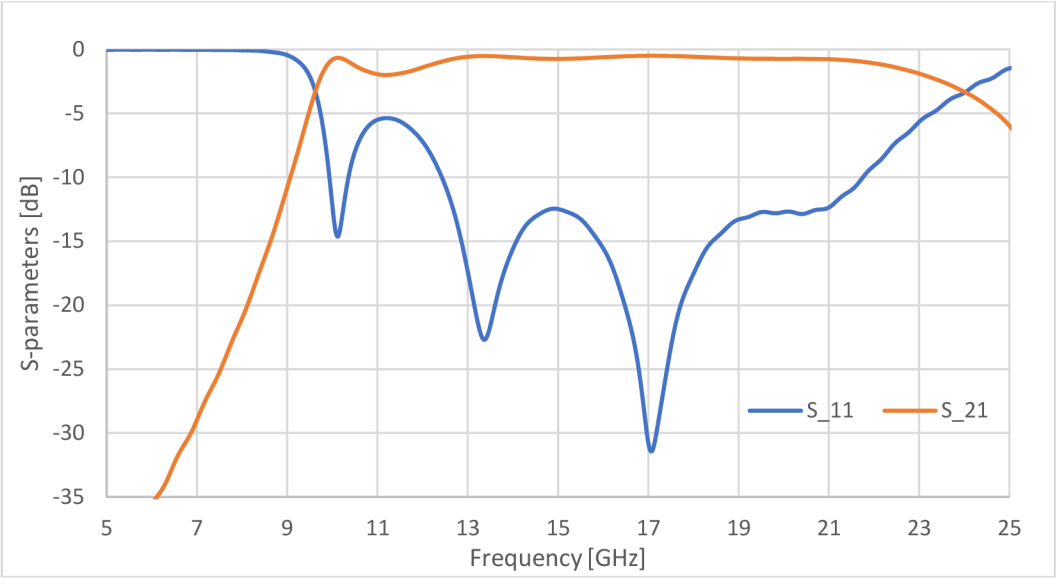

Fig. 5.9 S-parameters of SIW feed by coaxial probe

In order to achieve optimal value of S-parameters, the coaxial probe is placed at a distance λ/4 from the end of the waveguide. Position is then fine-tuned by offsetting the connector and inserting probe into the substrate. With the help of an electromagnetic simulator, the optimal position of probe was found so that the waveguide achieves the best possible value of transmission S_{21} and reflection coefficients S_{11}. Figure (5.10) compares S-parameters dependence on probe length.

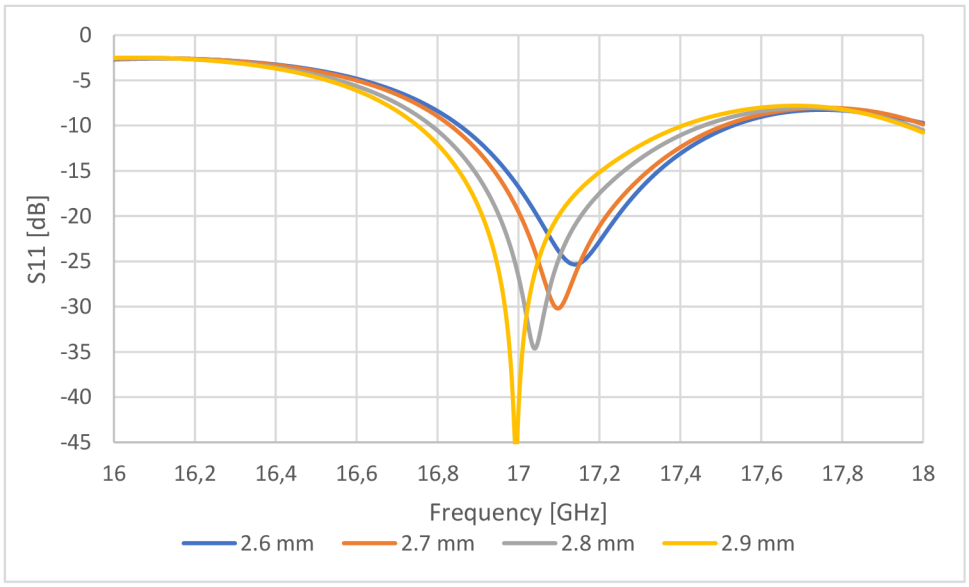

Fig. 5.10 Performance of SIW dependant on length of probe

The addition of a coaxial probe results in a degradation of both S_{11} and S_{22} parameters due to mismatched impedance between input and output port of the waveguide. Nevertheless, waveguide still meets the conditions for transmission with low attenuation S_{11} < -20db and S_{21} > -2dB (Fig. 5.10).

5.5 Waveguide filter

When designing filters within SIW, the same rules apply as for conventional rectangular waveguides. More on this in chapter 3.2. Tuning rectangular waveguide is often done by tunning pins however this solution encounters many limitations when used in SIW. The main limitation is the thickness of the substrate from which the waveguide is made. Tuning screw in this case can be moved only by few millimetres, which depending on the signal frequency propagating inside waveguide may not be enough to achieve sufficient results . In general, PIN diodes tuning is often used [16], but this solution involves extra electronic components that further complicate filter design. Unlike passively operating tuning pins, pin diodes require additional power supply and control circuits.

-

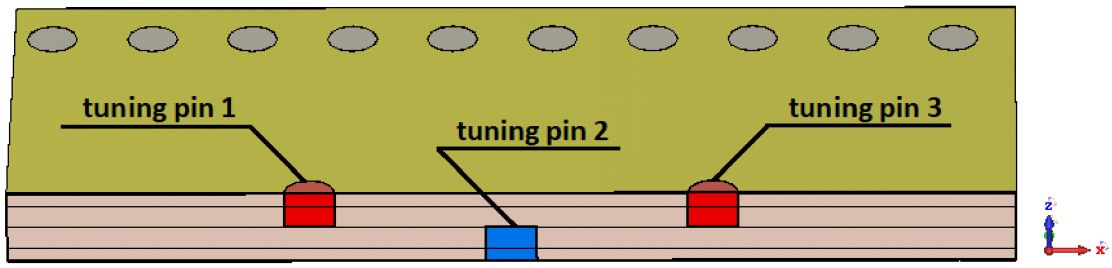

Fig. 5.11 Cross section of SIW filter using tunning pins

Figure (5.11) shows the proposed solution of the tuneable SIW filter. Tuning pins, two from the top side and one from the bottom side were placed along the waveguide x axis.

Depending on the depth of inserted tuning pin, a capacitive or inductive coupling is formed inside waveguide which affects the filtering properties. Figure (5.12) demonstrates the gradual change of resonant frequency over a wide range of frequencies from 15 to 19 GHz. Reflection coefficient S_{11} reached at least -28 dB in all cases.

Diameter and spacing of individual tuning pins also affect tuning performance of the waveguide, but the primary tuning parameter is the length of inserted tuning pin. Accuracy of resonant frequency is highly dependent on the step with which we are able to insert this pin into the waveguide. Since the waveguide will be manufactured as part of an antenna (Chapter 6), pins will be replaced by bolts with metric thread. Distance of individual pins was set by electromagnetic simulator to 4,1 mm so that the reflection coefficient S_{11} reaches stable values over the entire tuned frequency band (Fig. 5.12).

Minimum distance between the pins was also limited by the size of the nuts in which the tuning screws will be positioned.

-

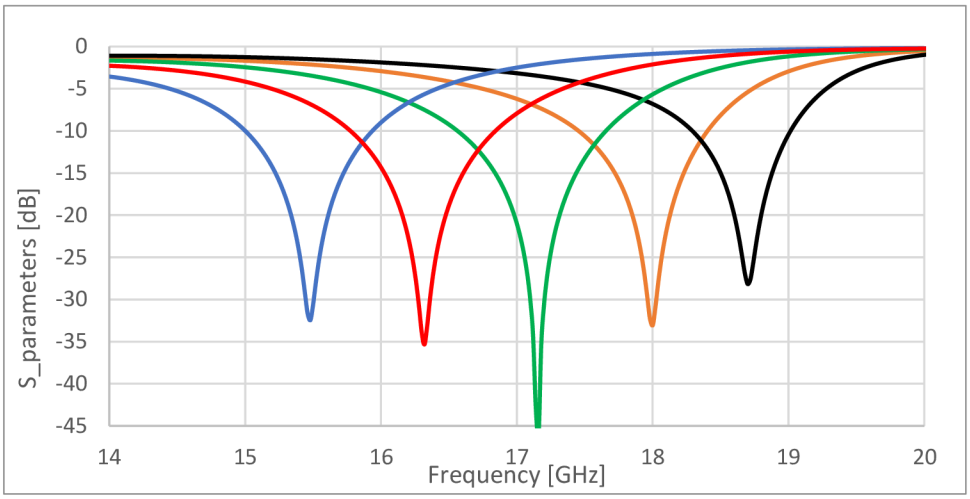

Fig. 5.12 Change of resonant frequency in SIW caused by tuning pins

5.6 Design of Horn SIW antenna

Antenna designed in such a way exhibits low efficiency due to mismatched impedance between the waveguide end and free space. Impedance sharply changes from 26 Ω at the end of the waveguide to a free space impedance of 360 Ω causing low performance of an antenna.

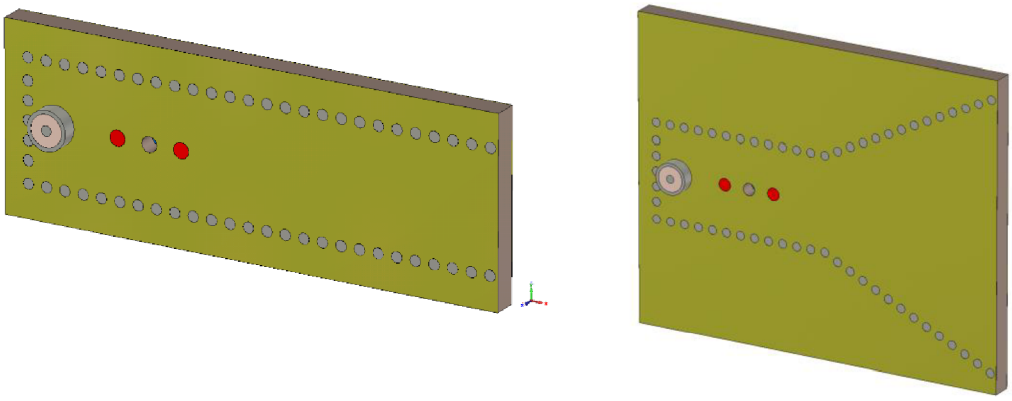

a) b)

Fig. 5.13 a) Tuneable SIW antenna b) Tuneable SIW horn antenna

In order to improve efficiency of antenna, the end of the waveguide is gradually expanded which results in a gradual transformation of impedance at the antenna end, thus increasing the overall efficiency of the antenna. Horn antenna walls are constructed with the same metallic vias as in the SIW.

Length of the horn antenna affects maximum achieved gain, and the angle that the antenna forms with the main axis of the waveguide affects directivity of antenna [18]. Therefore, final antenna dimensions depend on the desired antenna parameters.

Figure (5.14) demonstrates possibility of tuning operating frequency in the specified frequency range from 17 to 17.3 GHZ. Table (5.4) shows length of tuning pins for different resonant frequencies. Reflection coefficient S11 stayed below -35 dB and vswr does not exceed the value of 1.033 for all tuned frequencies, indicating proper impedance matching. Bandwidth of designed antenna does not change and remains stable at 700 MHz.

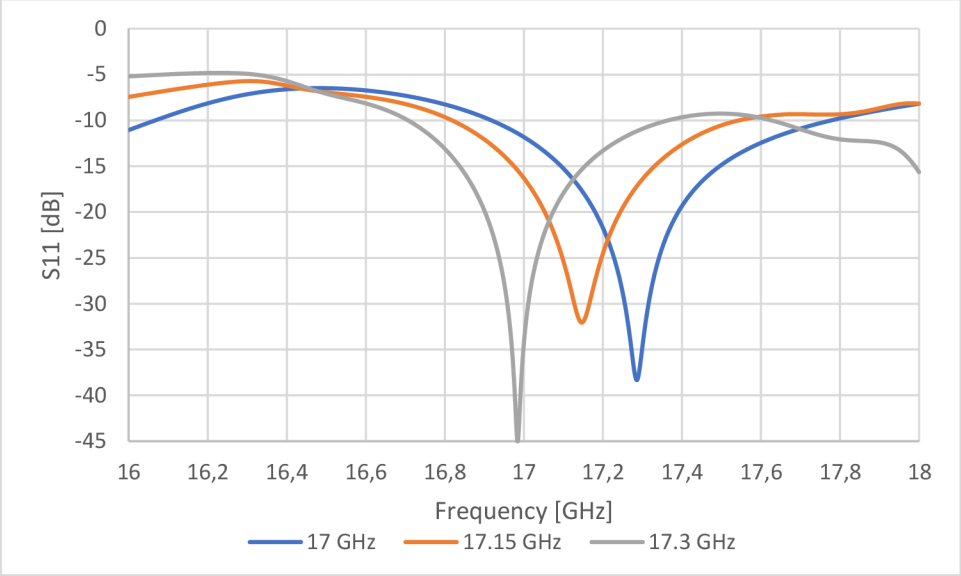

Fig. 5.14 Changes in resonant frequency of SIW horn antenna

Table 5.4 Length of tuning pins for SIW horn antenna

-

Frequency [GHz]	Pin 2 [mm]	Pin 1-3 [mm]
17	1.07	1.62
17.15	0.74	1.26
17.3	0.48	1.18

5.6.1 Improving Gain of proposed antenna

The antenna designed in subsection chapter 5.6 achieves very small directivity and gain of only 2.49 dBi with a beamwidth HPBW of 192.6° in the E plane and 35.5° in the H

plane. The shape of the radiation pattern is omnidirectional which is not desirable for this type of antenna. To improve these parameters, a technique is used where a resonator or a dielectric lens [18] formed by a substrate is placed in front of the antenna.

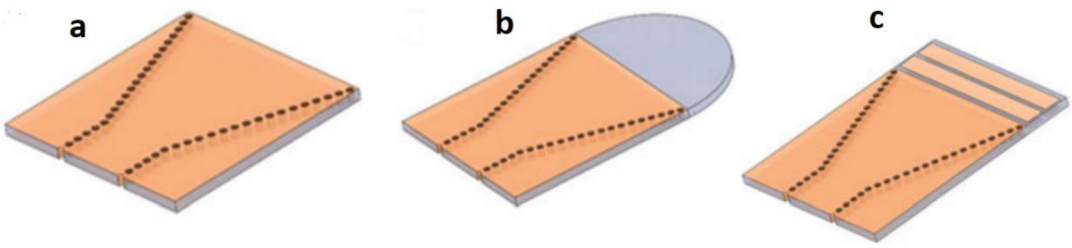

Fig. 5.15 a) SIW horn antenna b) dielectrically loaded SIW horn antenna c) SIW horn antenna with dielectric resonator [4]

Figure (5.15) demonstrates several cases of dielectrically loaded Horn antennas with elliptical and rectangular dielectric loading. From Figure (5.16) we can observe that as the length of the resonator increases the total antenna gain increases but only to a certain point. As we continue to increase the length of the dielectric load the electromagnetic waves start to become absorbed in the substrate instead of being radiated to the free space, thus lowering the gain.

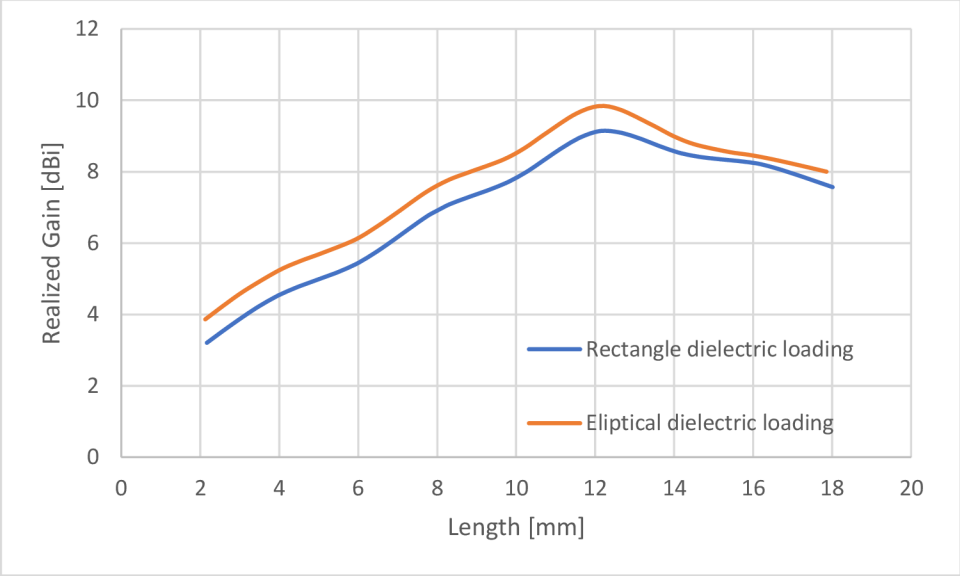

Fig. 5.16 Gain vs Length of dielectric loading

Proposed resonator for the SIW Horn antenna shown in Figure (5.17) consists of a rectangular block of substrate with the same parameters as the SIW. On its bottom and top sides are placed copper strips which purpose is to guide the electromagnetic wave and in doing so shape the directional characteristic of the antenna.

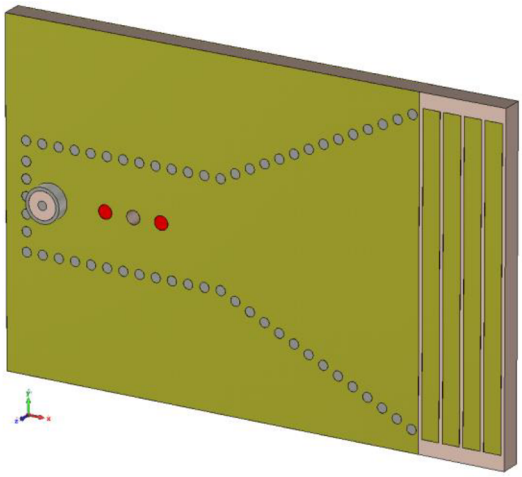

Fig. 5.17 Designed SIW horn antenna with dielectric rectangular loading

A reasonable length of resonator was determined to obtain acceptable radiation pattern. Figures (5.18 - 5.19) shows comparison of the radiation pattern in the E and H planes for an antenna with and without a dielectric resonator. In the E plane beamwidth dropped from 192.6° to109.4°. Thereby increasing gain to 10.5dbi from 2.49dbi.

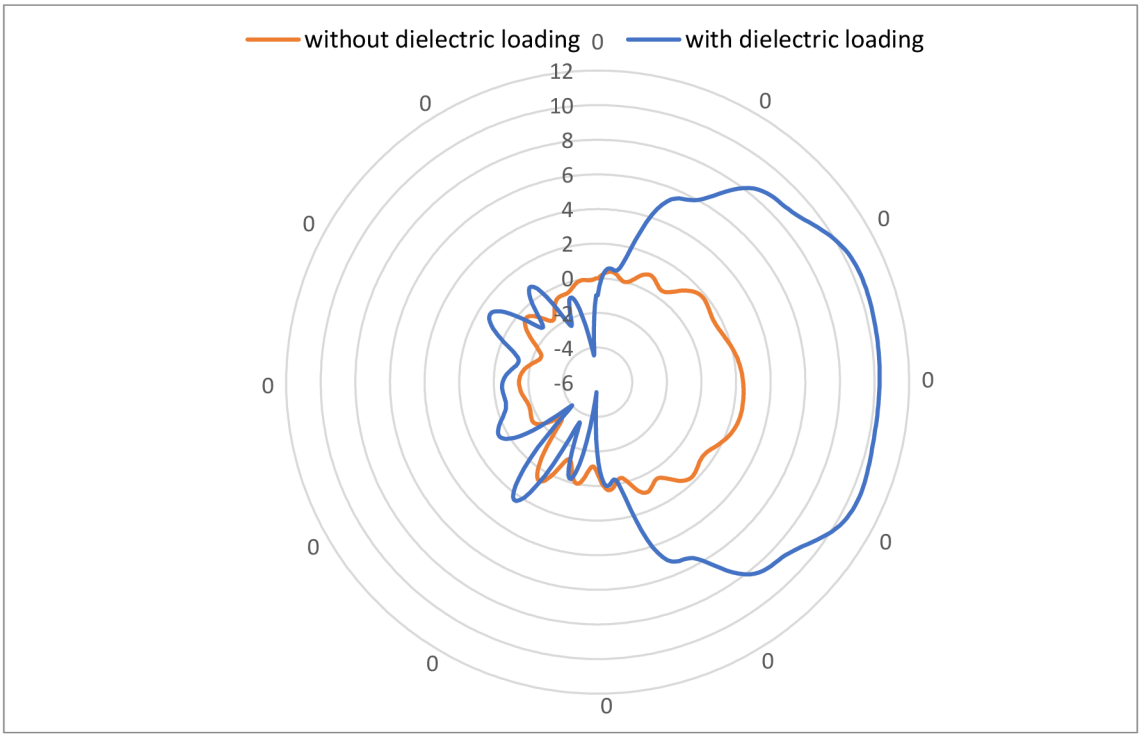

Fig. 5.18 Radiation pattern H plane

Beam width in H plane was reduced from 35.5° to 24.4°. Dielectric lens led to significant suppression of back lobe radiation by 6.9 dBi compared to the antenna without resonator.

Addition of the resonator also did not affect the filtering capability of the antenna which can still be tuned as demonstrated by figure (5.14)

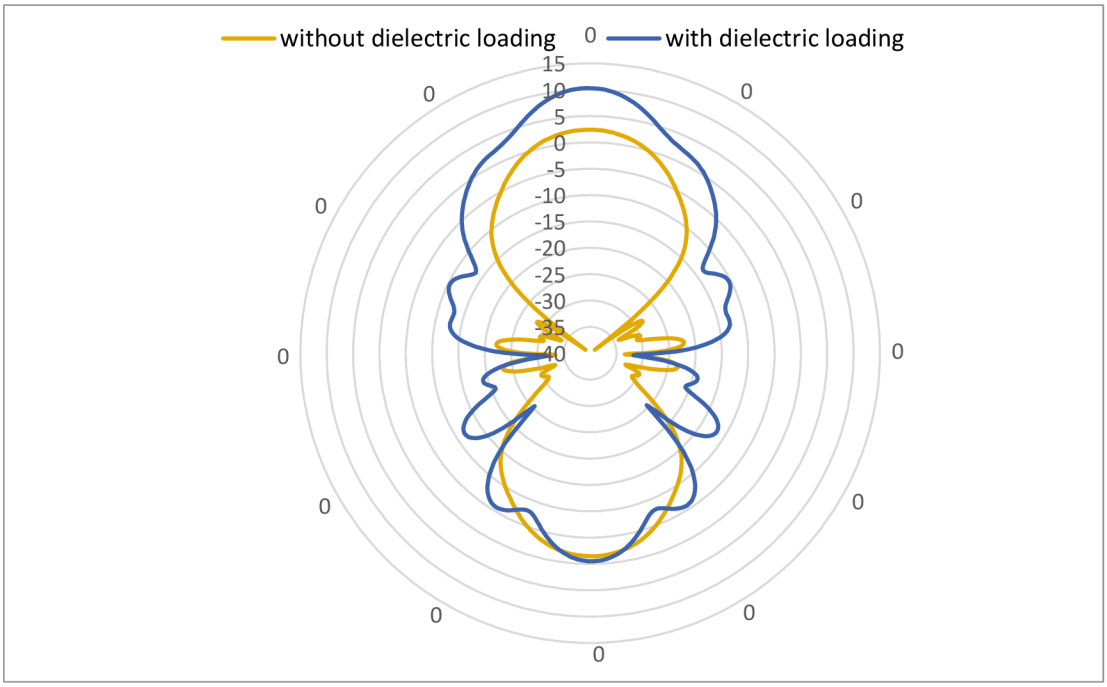

Fig. 5.19 Radiation pattern H plane

6. MANUFACTURING OF SIMULATED ANTENNA

Prior to the actual manufacture of the antenna designed in Chapter 5, it was necessary to make several changes to the antenna design to meet the manufacturing tolerance required for the UREL workshops where the antenna was manufactured. Since the sensitivity of the antenna tuning depends on the fineness of tuning screw thread, and the antenna bandwidth depends on the substrate thickness the two types of antennas were initially considered for fabrication.

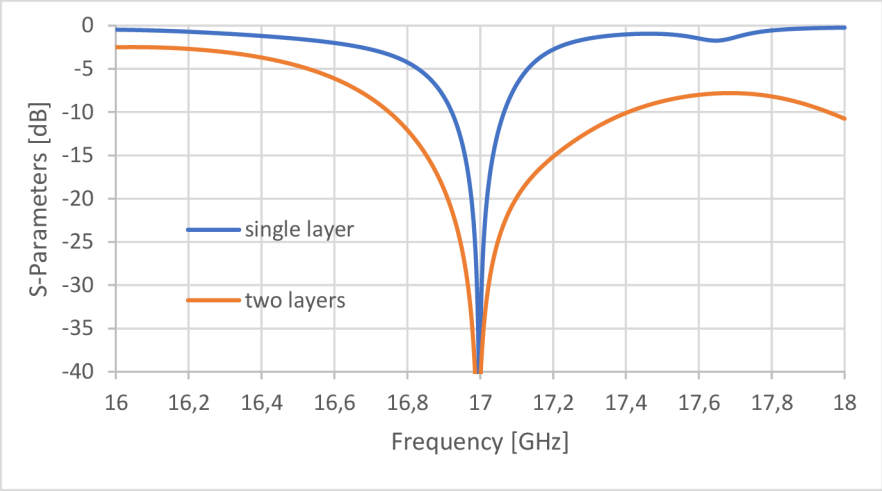

Fig. 6.1 Bandwidth comparison between single and multilayer antenna

First prototype assumed antenna fabrication from a single layer of CuCald 217 substrate. The proposed antenna achieves a low bandwidth (Fig. 6.1), but the antenna design is very simple. Problem with single layer antenna is that by using standard M2 screws with thread pitch of 0.4mm, tuning step might not be fine enough. For this reason a second version of the antenna was proposed. The antenna body consisted of two layers of CuClad 217 substrates, glued with double-sided tape and mechanically secured with additional screws to prevent movement between the plates, as shown in Fig. 6.2).

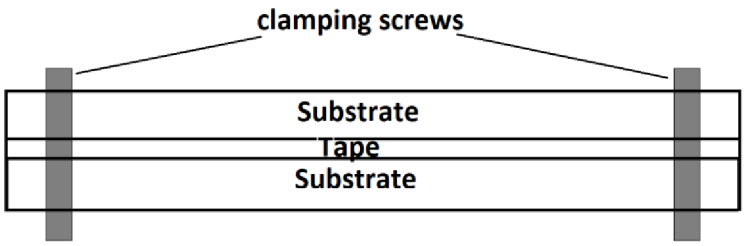

Fig. 6.2 Gain vs Length of dielectric load

The main advantage of this solution is that a higher antenna bandwidth is achieved (Fig. 6.1). The thickness of the entire antenna has been increased to 3.04mm. In this case, a standard pitch 0.4 mm screw will form a fine enough travel for antenna tuning.

However, this solution is much more difficult to manufacture, the alignment of the two substrates must be precise, and there is also risk of individual vias breaking when mechanically connecting two substrates together, which leads to lower efficiency.

Table 6.1 Substrate parameters comparison

Substrate	ε_r [-]	tan δ [-]	Height [mm]	Cladding thickness[µm]
CuClad217	2.17	0,0009	1.52	17.5
Rogers 5870	2.33	0.0012	3.18	35

For the above reasons, the third variant was chosen for final production, replacing the CuClad 217 substrate with Roggers 5870 with a dielectric constant of e_r = 2.33 and dileectric loss of δ = 0.0012. A comparison of the two substrates is shown in Table (6.1). The characteristics of the two substrates are very similar, so minimal changes to the antenna design were required. The final dimensions of the antenna are shown in (Fig. 6.3).

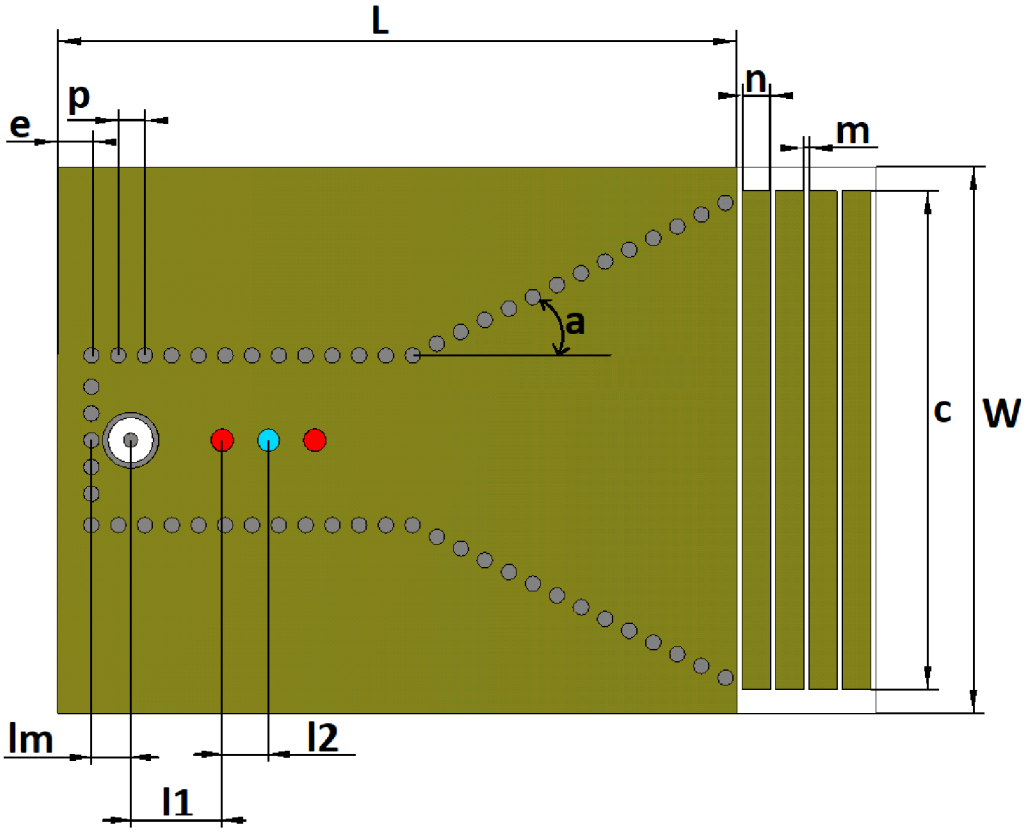

Fig. 6.3 Final dimension of manufactured antenna

Table 6.2 Dimensions of fabricated antenna

l1 [mm]	8.42	**c [mm]**	44.7
l2 [mm]	4.15	**W [mm]**	48.95
lm [mm]	4,08	**n [mm]**	2.5
e [mm]	3.05	**m [mm]**	0.5
p [mm]	2.4	**a [°]**	26
L [mm]	60.9		

Completed antenna is shown in (Fig. 6.4a) with overall dimensions of 7.3 cm x 4.9 cm and fitted with an SMA connector with the feed pin filled down to the value determined by simulation (2.9 mm - 3 mm). A nylon-insert nuts were soldered in place of the tuning pins to minimize unwanted movement of the adjustment screws within the waveguide during antenna operation. Standard M2 metric bolts with thread pitch of 0.4mm were used for tuning pins. Bolts with finer thread pitch of 0.25 mm would increase the tuning sensitivity however such bolts and nut are not commonly available. Fully assembled antenna is shown in (Figure 6.4 b).

a) b)

Fig. 6.4 a) Fabricated antenna b) Antenna with tuning pins and SMA connector

7. COMPARISON OF SIMULATED AND MEASURED RESULTS

Two antenna samples were manufactured, due to the reason than not always all the vias were successfully coated with copper layer. Antenna with larger number of successful vias was chosen for the final measurement. The measurement was carried out in two steps, measuring the S-parameters on vector network analyser and measuring the radiation pattern of the antenna in anechoic chamber.

7.1 Measuring S-parameters

The S-parameters were measured on a vector network analyser (Agilent Technologies E5071C) at the Department of Radioelectronics. Antenna was attached to the vector network analyser via a coaxial cable with SMA connectors. Tuning screws were gradually adjusted in order to achieve desired resonant frequencies. The figure (Fig. 7.1) demonstrates a comparison of the measured and simulated values of reflection coefficient S_{11}.

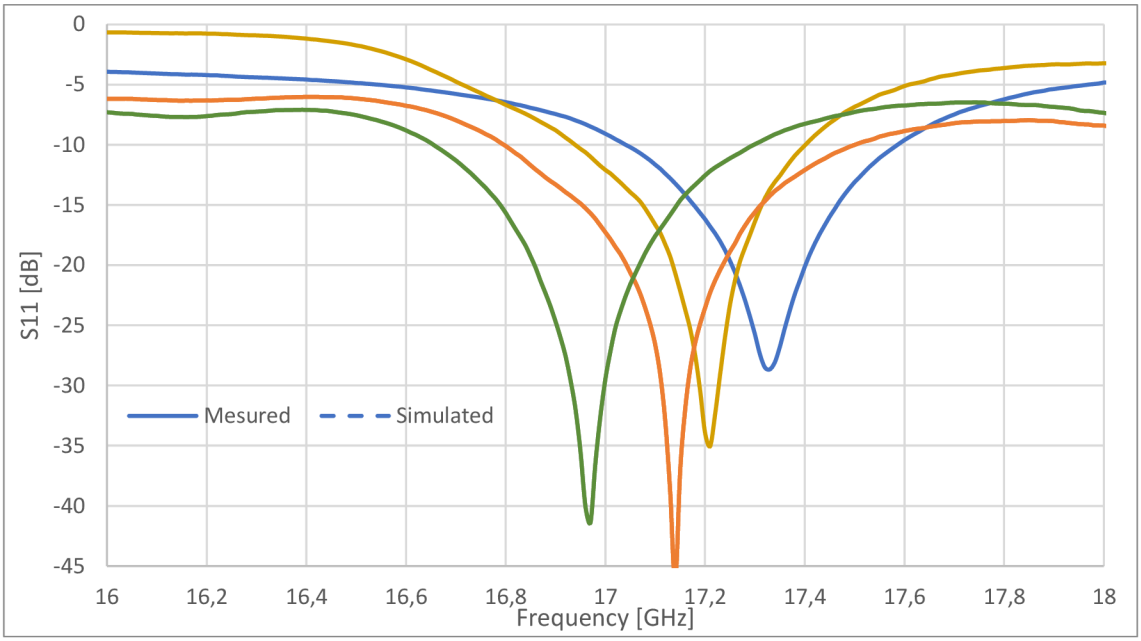

Fig. 7.1 Simulated and measured reflection coefficient S_{11} for frequency tuning

The antenna under test could be continuously tuned by tuning pins in the specified frequency range from 17 to 17.3 GHz. The reflection coefficient S_{11} corresponds to the simulated values but tends to decrease as the frequency increases. The bandwidth at each resonant frequency differs from the simulated values by approximately 50 to 100 MHz

Figure (7.2) demonstrates the change of the antenna bandwidth independent of the resonant frequency. However, during measurement slight shift of the resonant frequencies by less than 50MHz was observed. Antenna during bandwidth tuning was very sensitive to the movement of the tuning pins. This behaviour could be suppressed by using screws with a finer thread.

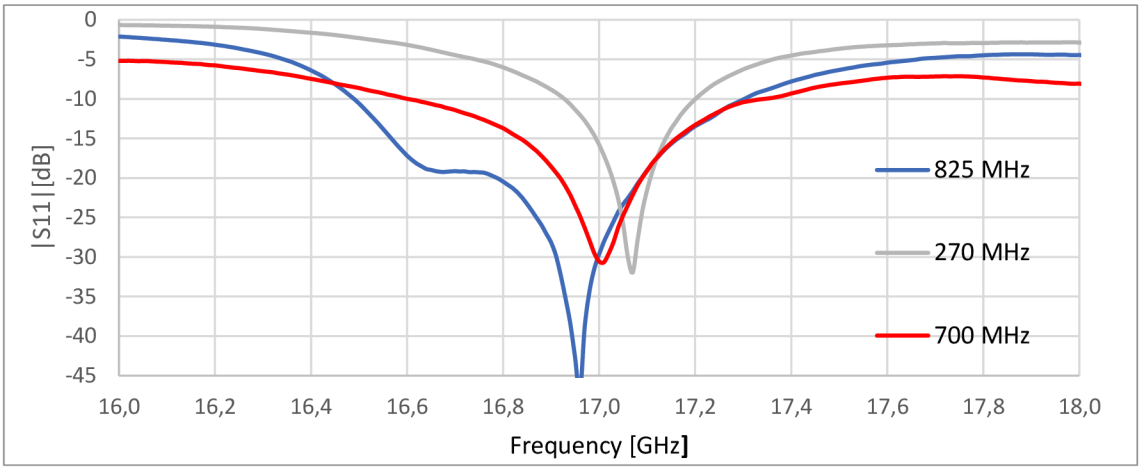

Fig. 7.2 Simulated and measured reflection coefficient S_{11} for bandwidth tuning

Due to manufacturing reasons, it was not possible to drill holes of a certain depth into the substrate and therefore all holes were drilled through the entire substrate. The resulting holes leaked some of the electromagnetic energy and reduced the performance of the antenna. During the measurements, the holes were covered with conductive copper tape. This modification had the effect of increasing the efficiency of the antenna as well as suppressing parasitic resonances (Fig. 7.3)

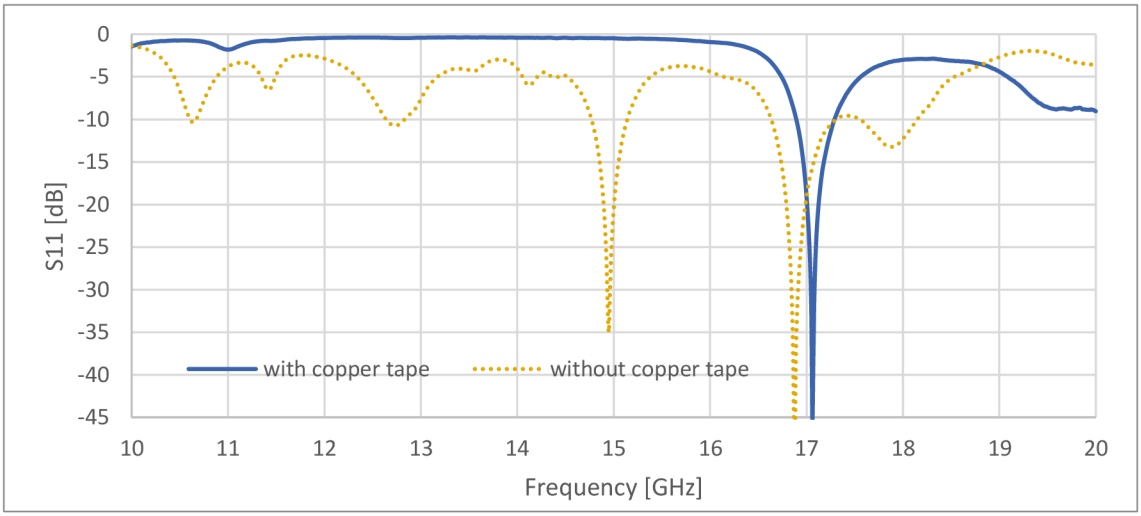

Fig. 7.3 Eliminating resonanceis with copper tape

-

7.2 Radiation pattern measurement

Radiation patterns were measured in an anechoic chamber in the laboratory of the Department of Radio Electronics. The layout of antenna under test is depicted in (Fig 7.4) Measured antenna was placed on a rotating base whose rotation was controlled by a step motor connected to the control PC. Receiving horn antenna together with antenna under test were connected to vector network analyser which than sends measured data back to the computer. To obtain full radiation pattern, measured antenna was rotated together with its support structure by 360° Which gave us measurement in E plane. Antenna was the placed perpendicular to the ground and again spun around the by 360° resulting in radiation pattern in H plane.

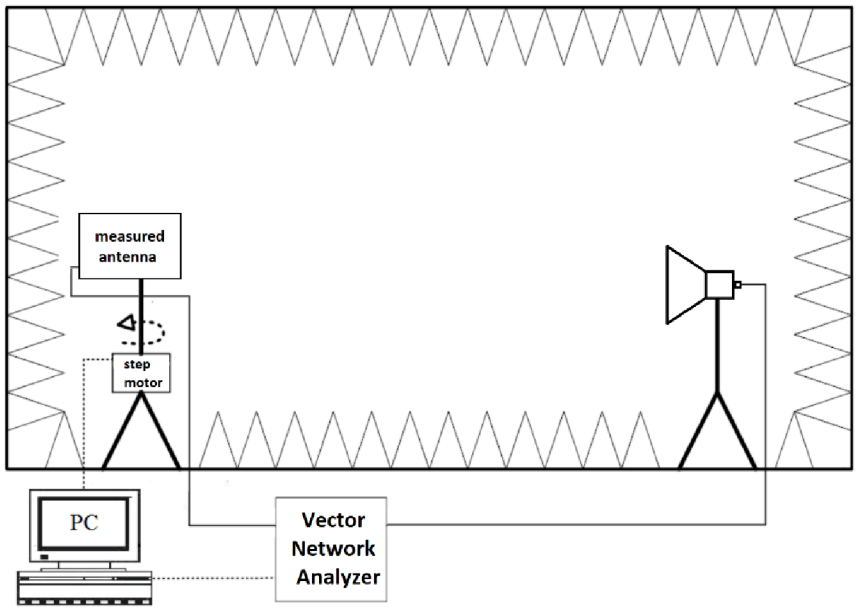

Fig. 7.4 Antenna placement in anechoic chamber

Figures (7.5 – 7.6) compares radiation pattern of simulated and measured antennas in both E and H plane at frequency of 17.1 GHz. From the figures is apparent that measured antenna reaches gain of 11.5 dBi which is 1 dB more than predicted by simulation. Measured antenna has also significantly higher suppression of backward radiation up to -35 compared to simulated values. Direction of main lobe was offset by 2° from centre line of the antenna, however this could be the result of not perfectly levelling the antenna in its support stand.

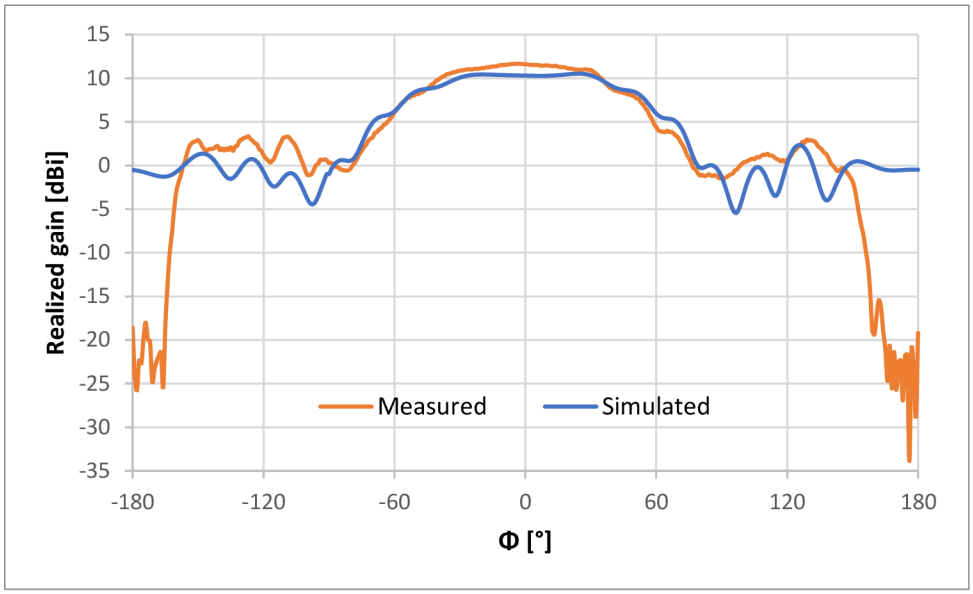

Fig. 7.5 Simulated and measured characteristics at 17.1 GHz in E plane

-

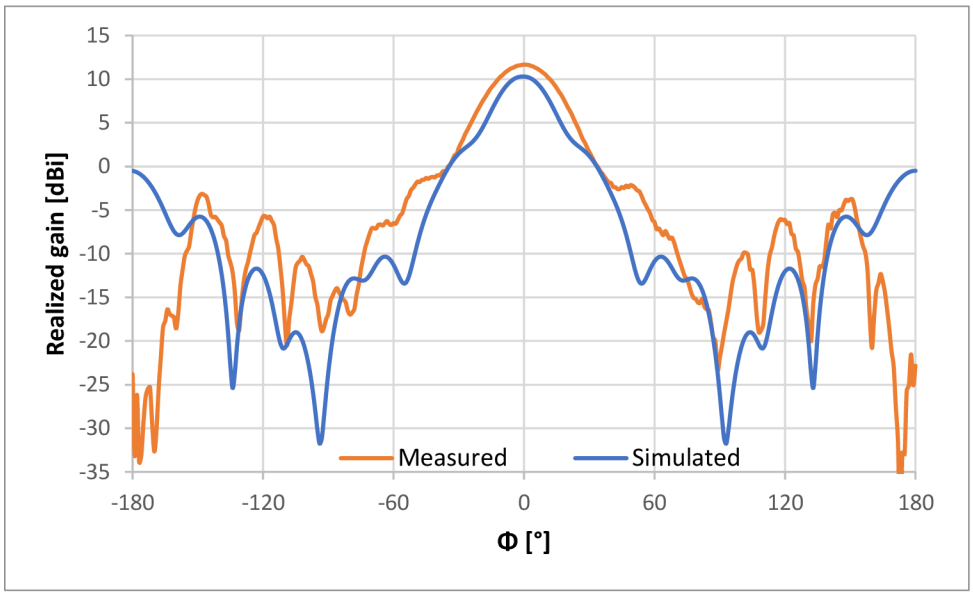

Fig. 7.6 Simulated and measured characteristics at 17.1 GHz in H plane

8. CONCLUSION

This project focuses on validating filtering function of antenna proposed in research paper [1]. Gained knowledge was later used for design and manufacturing filtering SIW antenna for use in HIPERLAN.

Tthesis begins by verifying the correctness of the proposed filtering antenna in article [1]. In this article base of the antenna consists of a WR90 cavity waveguide into which several cylindrical passive resonators are inserted. These cylinders fulfil the role of fine threaded tuning screws, which are used in design in case of manufacturing waveguide filter antenna. Cylinders are divided into two groups, first group of three cylinders sets the resonant frequency. While the second group of four cylinders sets quality factor of feeding and radiating port. With ability to adjust quality factor, we can ensure that antenna will have same parameters across the full range of operating frequencies from 9 to 10 GHz. In case of a higher order antenna, these cylinders also ensure weak coupling between resonant and coupling cylinders.

After creating model according to the template in paper [1], antenna was simulated in electromagnetic simulator HFSS. Afterwards, frequency and bandwidth tuning function was independently verified. Achieved results are provided in Chapter 3. For first order filtering antenna, there was a shift of resonant frequencies by 20 MHz, also reflection coefficient decreased by 10 dB on average. Gain of antenna was 7.5 dBi compared to reported value of 8.1 dBi, for each of tuned frequencies. Antenna radiated a linearly polarized wave with a directivity of 7.7 dB and HPBW (Half Power Beam Width) of 63°.

To increase antenna selectivity, article proposes a third-order filtering antenna with a higher number of tuning pins. Antenna retains ability of resonant frequency tuning and bandwidth tuning. However, using tuning pins, one cannot change the gain or directivity of antenna. In order to improve these parameters, Chapter 4 proposes modification of this antenna where horn antenna is placed at the end of the filtering waveguide.

With commercially available antenna models, a pyramidal horn with a reported gain of 15dBi was selected for experimental validation. This antenna was modelled in CST Microwave studio and placed at the end of the filtering waveguide.

The experiment showed that filtering part of antenna retains ability of frequency tuning, however, there is slight asymmetry in the reflection coefficient characteristic due to which tuned bandwidth is decreased. This asymmetry can be suppressed by using a tuning pin responsible for tuning quality factor *Qr*. Simulated gain was 14.9 dBi and beamwidth (HPBW) reached 34°in H-plane and 32°in E-plane.

Second half of the master's thesis focuses on the possibility of converting filtering antenna based on cavity waveguides into an antenna integrated into the substrate. First step was to properly design the SIW to ensure the transmission of electromagnetic energy with the lowest possible attenuation. After achieving this goal, a filter was implemented in the waveguide using metric M2 bolts which were used to tune the resonant frequency.

SMA connector was used to feed the waveguide thus creating simple open-ended waveguide antenna.

To increase the radiation efficiency, the end of antenna was widened to ensure a gradual change of impedance between the waveguide and free space. The simulation showed that the antenna has an omnidirectional characteristic in the E plane which is not desirable. In order to increase the directivity and gain, a dielectrically loaded block was placed in front of the antenna. By doing so gain of the main lobe was increased by 8 dB while the back lobe was significantly supressed.

After the completion of the antenna design, two prototypes of the antenna were produced in the workshops of UREL. Antenna with the larger number of successful vias was fitted with a connector and tuning screws.

The subsequent measurement of the antenna with a vector network analyser revealed that the antenna can be tuned in the defined frequency range spanning from 17 to 17.3 GHz as predicted by the simulation. It was also possible to tune the antenna bandwidth to the desired value however fine-tuning bandwidth would require screws with smaller thread pitch.

The radiation pattern in the E and H planes was verified by measurements in an anechoic chamber. The antenna achieved gain of 11.54 dB which is 1 dB higher compared to the simulated one. The fabricated antenna also significantly suppressed the back side radiation by up to 35 dB.

Master thesis proves that for the design of an antenna integrated into the substrate it is possible to apply the same design rules as in the case of a cavity waveguide-based antenna.

LITERATURE

[1] XIANG, Kai-Ran, Fu-Chang CHEN a Qing-Xin CHU. A Tunable Filtering Antenna Based on Coaxial Cavity Resonators. IEEE Transactions on Antennas and Propagation [online]. 2022, 70(5), 3259-3268 [cit. 2022-12-26]. ISSN 0018-926X. Avaliable from:10.1109/TAP.2021.3137516

[2] BALANIS, Constantine A. Antenna theory: analysis and design. Fourth edition. Hoboken, New Jersey: Wiley, [2016]. ISBN 978-1-1186-4206-1.

[3] Phase 2 Microwave [online]. Copyright © [cit. 30.12.2022]. Avaliable from: http://www.phase2mw.co.uk/images/docs/Waveguide_guide.pdf

[4] Folgerø, Kjetil. (2001). Step-by-step procedure for design of waveguide filters with HFSS. [online]. Avaliable from: https://www.researchgate.net/publication/282664113_Step-by-step_procedure_for_design_of_waveguide_filters_with_HFSS

[5] Antenna Theory - Horn. [online]. Copyright © Copyright 2022. All Rights Reserved. [cit. 30.12.2022 Avaliable from: https://www.tutorialspoint.com/antenna_theory/antenna_theory_horn.htm#

[6] [online]. [cit. 30.12.2022] Avaliable from: http://www.pasternack.com/wr-90-waveguide-standard-gain-horn-antenna-15-dbi-n-pewan090-15elnf-p.aspx

[7] HONG, Tao, Shuli ZHENG, Rongke LIU a Weiting ZHAO. Design of mmWave Directional Antenna for Enhanced 5G Broadcasting Coverage. Sensors [online]. 2021, 21(3) [cit. 2022-12-30]. ISSN 1424-8220. Avaliable from: doi:10.3390/s21030746

[8] XIANG, Kai-Ran, Fu-Chang CHEN a Qing-Xin CHU. A Tunable Filtering Antenna Based on Coaxial Cavity Resonators. IEEE Transactions on Antennas and Propagation [online]. 2022, 70(5), 3259-3268 [cit. 2022-12-31]. ISSN 0018-926X. Avaliable from: doi:10.1109/TAP.2021.3137516

[9] TOMASSONI, Cristiano a Giuseppe MACCHIARELLA. A New Resonant Coupling Structure for Inline Waveguide Filters with Transmission Zeros. In: 2021 IEEE MTT-S International Microwave Filter Workshop (IMFW) [online]. IEEE, 2021, 2021-11-17, s. 297-299 [cit. 2022-12-31]. ISBN 978-1-7281-6804-3. Avaliable from: doi:10.1109/IMFW49589.2021.9642303

[10] HOFT, M., T. MAGATH, O. BARTZ a S. BURGER. Corner rounding for increased quality factor of cavity resonators. In: 2005 Asia-Pacific Microwave Conference Proceedings [online]. IEEE, 2005, s. 1-4 [cit. 2022-12-31]. ISBN 0-7803-9433-X. Avaliable from: doi:10.1109/APMC.2005.1606272

[11] WU, Ke, D. DESLANDES a Y. CASSIVI. The substrate integrated circuits - a new concept for high-frequency electronics and optoelectronics. In: 6th International Conference on Telecommunications in Modern Satellite, Cable and Broadcasting Service, 2003. TELSIKS 2003 [online]. IEEE, 2003, 2003, P-III [cit. 2023-05-20]. ISBN 0-7803-7963-2. Avaliable from: doi:10.1109/TELSKS.2003.1246173

[12] FENG XU a Ke WU. Guided-wave and leakage characteristics of substrate integrated waveguide. IEEE Transactions on Microwave Theory and Techniques [online]. 2005, 53(1), 66-73 [cit. 2023-05-20]. ISSN 0018-9480. Avaliable from: doi:10.1109/TMTT.2004.839303

[13] CuClad® 217 Laminates. Helping power, protect and connect our world [online]. Copyright © 2023 Rogers Corporation. All Rights Reserved. [cit. 20.05.2023]. Avaliable from: https://www.rogerscorp.com/advanced-electronics-solutions/cuclad-series-laminates/cuclad-217-laminates

[14] VYSKOČIL, J. Filtr na bázi vlnovodu integrovaného do substrátu [online]. Brno, 2011. 50 s. Diplomová práce. FEKT VUT Brno. Avaliable from: http://www.vutbr.cz/studium/zaverecne-prace?zp_id=39393.

[15] MORINI, Antonio, Marco FARINA, Cristian CELLINI, Tullio ROZZI a Giuseppe VENANZONI. Design of Low-Cost non-radiative SMA-SIW Launchers. In: 2006 European Microwave Conference [online]. IEEE, 2006, 2006, s. 526-529 [cit. 2023-05-20]. ISBN 2-9600551-6-0. Avaliable from: doi:10.1109/EUMC.2006.281426

[16] S, Ganaraj P, Koushik GUHA a M KAVICHARAN. Tunable Quarter Mode Substrate Integrated Waveguide filter for 5G communication. In: *2022 IEEE Silchar Subsection Conference (SILCON)* [online]. IEEE, 2022, 2022-11-4, s. 1-5 [cit. 2023-05-20]. ISBN 978-1-6654-7100-8. Avaliable from: doi:10.1109/SILCON55242.2022.10028907

[17] PASIAN, Marco, Maurizio BOZZI a Luca PERREGRINI. A Formula for Radiation Loss in Substrate Integrated Waveguide. *IEEE Transactions on Microwave Theory and Techniques* [online]. 2014, **62**(10), 2205-2213 [cit. 2023-05-20]. ISSN 0018-9480. Avaliable from: doi:10.1109/TMTT.2014.2341663

[18] DJERAFI, Tarek, Ali DOGHRI a Ke WU. Substrate Integrated Waveguide Antennas. In: CHEN, Zhi Ning, ed. *Handbook of Antenna Technologies* [online]. Singapore: Springer Singapore, 2014, 2015-09-09, s. 1-60 [cit. 2023-05-20]. ISBN 978-981-4560-75-7. Avaliable from: doi:10.1007/978-981-4560-75-7_57-1

SYMBOLS AND ABBREVIATIONS

Abbreviations:

RF	Radio Frequency
BER	Bit Error Ratio
SNR	Signal to Noise ratio
IEEE	Institute of Electrical and Electronics Engineers
MIL	United States Military
EIA	Electronic Industries Alliance Standards
IEC	International Electrotechnical Commission
HPBW	Half Power Beam Width
SIW	Substrate Integrated Waveguide
TE	Transverse Electric
TM	Transverse Magnetic
SIW	Substrate Integrated Waveguide
PEC	Perfect Electric Conductor

Symbols:

f_c^{TE10}	cut-off frequency for TE10 mode	(Hz)
f_c^{TE20}	cut-off frequency for TE20 mode	(Hz)
a	longer side of rectangular waveguide	(mm)
b	shorter side of rectangular waveguide	(mm)
c	speed of light	(m/s)
m,n	waveguide mode numbers	(-)
λ	Wavelength	(m)
λ_c	Wavelength of cut-off frequency	(m)
λg	Wavelength inside waveguide	(m)
ε	Permittivity	(F/m)
ε_r	Relative permittivity	(-)
μ	Permeability	(H/m)
μr	Relative permeability	(-)
δ	Dielectric constant	(-)

dBi	Decibel related to isotropic antenna
GHz	Gigahertz
MHz	Megahertz
mm	Millimetre
dB	Decibel

LIST OF APPENDICES

Appendix A – Detail of manufactured antenna

A.1 Top side

A.2 Bottom side

Appendix B – Detail of manufactured antenna

A.3 Measuring antenna S-parameters

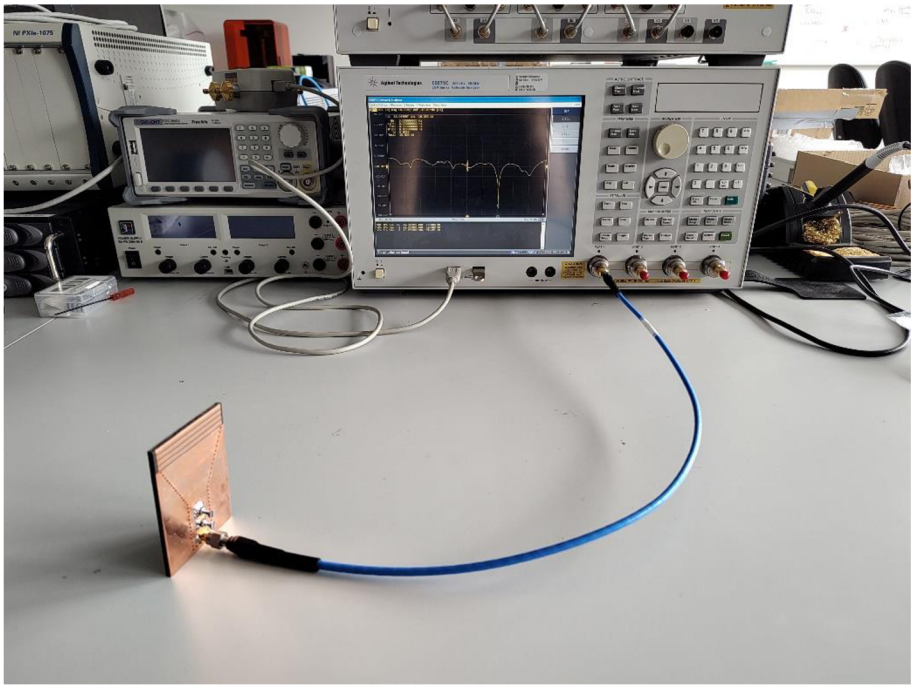

A.4 Measuring antenna radiation pattern